Int.J.Curr.Microbiol.App.Sci (2019) *8*(1): 1517-1546

International Journal of Current Microbiology and Applied Sciences
***ISSN: 2319-7706* Volume 8 Number 01 (2019)**
Journal homepage: http://www.ijcmas.com

Original Research Article https://doi.org/10.20546/ijcmas.2019.801.161

Multivalent Interactions of Nano-spaced Dimers of N-acetylneuraminic Acid Analogues Complex with H5N1 Influenza Viral Neuraminidase and Haemagglutinin - A Molecular Dynamics Investigation

J. Jino Blessy[1], D. Jawahar[2] and D. Jeya Sundara Sharmila[3*]

[1]Department of Bioinformatics, Karunya University, Karunya Nagar, Coimbatore-641 114, Tamil Nadu, India
[2]Directorate of Natural Resource Management, Tamil Nadu Agricultural University, Coimbatore-641003, Tamil Nadu, India
[3]Department of Nano Science and Technology, Tamil Nadu Agricultural University, Coimbatore-641003, Tamil Nadu, India

**Corresponding author*

Keywords

N-acetylneuraminic acid analogues, H5N1 influenza A virus, Neuraminidase, Haemagglutinin and Molecular dynamics simulation

Article Info

Accepted:
12 December 2018
Available Online:
10 January 2019

A B S T R A C T

Design of multivalent ligand is significant in restraining the interaction involved in the binding of influenza virus to its host cell. This molecular dynamics (MD) simulation study aims to study the mode of binding of dimeric NeuNAc analogues coupled by different nano-spacers into the multimeric binding sites of neuraminidase and haemagglutinin of influenza A H5N1 virus. In total, 80 NeuNAc analogue dimers were modeled and docked against the binding sites of neuraminidase and haemagglutinin. The top scoring complexes such as neuraminidase – 2-keto-3-deoxy-D-glycero-d-galacto-nononic acid (or KDN) dimer coupled by 1-nano-linker, neuraminidase – KDN dimer linked by CH-C1 nano-spacer, haemagglutinin – KDN dimer connected by CH-C1 nano-spacer and haemagglutinin – KDN dimer joined by CH-N1 nano-spacer were taken in for the conformational investigation by molecular dynamics (total 80ns) in aqueous environment. The potential energy profile, RMSD, RMSF, protein – ligand contacts and intermolecular hydrogen bond interactions suggest that the complexes were stable throughout the trajectory of MD simulations. The ligand torsion report was calculated for each rotatable bond of dimers of NeuNAc analogues which were bound to target proteins such as neuraminidase and haemagglutinin. The binding energy and conformational study of the complexes reveal that the nano-spacer coupled dimers of NeuNAc analogues may be used as potential candidates for designing multivalent drugs to inhibit neuraminidase and haemagglutinin and perhaps to prevent the viral spread.

Introduction

Multivalent interaction is one of the characteristic features exhibited in the binding of influenza virus to its host cell (1,2). Multivalent interaction plays a crucial role in carbohydrate recognition such as binding of multiple copies of carbohydrates or

oligosaccharides in the binding site of cell surface receptor protein (3, 4). Due to the significance of multivalency in biological systems, research efforts are rising to explore and rationalize the consequences of multivalent ligands to develop potentially new drugs (5, 6). Hence, a number of multivalent bioactive compounds predominantly dimeric forms of known therapeutic small molecules are being considered as drug candidates (7). Influenza haemagglutinin (HA) and neuraminidase (NA) are the target viral proteins which have multimeric binding site same as in human and simian immunodeficiency virus envelop proteins.

The virulence of avian H5N1 influenza A virus is highly pathogenic and a pandemic threat to humans and animals (8). In its pathogenesis, human H5N1 influenza disease differs significantly from seasonal human influenza viral disease. In H5N1 infection, the primary cause of death is owing to viral pneumonia. However, the virus also distributes beyond the respiratory tract with hypercytokinemia and leads to multi-organ failure (9)**.** The earlier *in-vitro, in-vivo* studies and clinical research recorded that various cytokines and chemokines including TNFα, IFN-α/β, IFN-γ, IL-6, IL-1, IL-8, MIP-1, MIG, IP-10, MCP-1 and RANTES were induced by H5N1 viruses that leads to H5N1 infection and cell death in both humans and animals (10-12)**.**

Influenza A virus consists of glycoproteins termed as haemagglutinin (HA) and neuraminidase (NA) along with M1 and M2 proteins to manage the entry and the exit of viral particle through the host cell receptors. In the host cell, haemagglutinin binds to the terminal sialic acid receptor on cell surface and the neuraminidase cleaves the terminal sialic acid from cell surface glycoconjugates to assist the viral shedding (13). It is reported that Influenza A virus haemagglutinin has 18 different antigens and neuraminidase has 11 different antigens (14). On the basis of nucleotide sequence phylogeny, haemagglutinin has divided into two groups, group_1 follows: H1, H2, H5, H6, H8, H9, H11, H12, H13, H16, and H17 and group_2 follows: H3, H4, H7, H10, H14, and H15 (15). Neuraminidase also forms two groups, group_1 follows N1, N4, N5, and N8 and group_2 follows: N2, N3, N6, N7, and N9. The viruses with several combinations of HA and NA subtypes are found in waterfowl of avian species which are the asymptomatic carriers (16).

N- acetylneuraminic acids (NeuNAc or Neu5Ac) are the most abundant sialic acids, the derivatives of neuraminic acid, a nine-carbon acidic monosaccharides commonly found in mammals and other vertebrates. They are found in the cell surface of glycan of glycoconjugates (gangliosides). They play a vital role in carbohydrate-protein recognition event leading to cell adhesion, cell-cell interactions and cell-virus recognition events. The NeuNAc inhibits sialic acid binding proteins such as sialoadhesins, selectins, and influenza hemagglutinins and may show potent antiviral, antibacterial and anti-inflammatory effects (17, 18).

In the present work, computational screening of NeuNAc analogue library against H5N1 viral neuraminidase and haemagglutinin was carried out using molecular docking techniques. In total, 153 NeuNAc analogues (Supplement Table 1) were screened against the H5N1 viral neuraminidase and haemagglutinin. The top five scoring NeuNAc analogues from neuraminidase-NeuNAc analogue complex and haemagglutinin- NeuNAc analogue complex were retrieved/selected for further dimerization study. Molecular modeling of homo dimerization of NeuNAc analogues were done in which eight nanospacers of

length in nano meter range were used separately to join the top five dock scoring NeuNAc analogues (Figure 1) resulting in a total of eighty homo NeuNAc analogue dimers that were screened against the neuraminidase and haemagglutinin using molecular docking. The conformational behavior of individual complexes such as neuraminidase-2-keto-3-deoxy-D-glycero-d-galacto-nononic acid (or KDN) dimer joined by 1-Linker (Figure 1), neuraminidase-KDN dimer coupled by CH-C1 nano-spacer, haemagglutinin- KDN dimer attached by CH-C1 nano-spacer and haemagglutinin- KDN dimer connected by CH-N1 nano-spacer were studied using molecular dynamics simulation each for 20ns.

Materials and Methods

Molecular docking

Molecular docking is a computational method to predict the favorable binding orientation between the receptor – ligand to form a favorable complex (19). The three dimensional structure of neuraminidase (PDB ID: 2HTQ) (16) and haemagglutinin (PDB ID: 4KDN_A) (20) were retrieved from protein data bank (PDB). The binding site residues of neuraminidase and haemagglutinin structure were referred from PDBsum database (16, 20) as follows: neuraminidase binding site residues are ARG118, GLU119, ASP151, ARG152, ARG156, TRP178, ILE222, ARG224, GLU227, ALA246, GLU276, GLU277, ARG292, TYR347, ARG371 and TYR406. The haemagglutinin binding site residues are TYR95, LEU133, GLY134, VAL135, SER136, SER137, TRP153, ILE155, HIS183, GLU190 and LEU194. Both the neuraminidase and haemagglutinin proteins were prepared, optimized and minimized using protein preparation wizard of Maestro v9.2 (21). The preparation of protein structure involves the following steps: (i) import the present protein structure from PDB into Maestro environment, (ii) to locate the water molecules or delete the water molecules, (iii) if the binding sites have dimer or multimer binding sites or multiple chains, remove the duplicate chains, (iv) adjust the protein structure for metal ions and cofactors, (v) check the ligand bond orders and formal charges, (vi) adjust the ionization and tautomerization state, (vii) protein preparation is the final step to refine the protein structure and (viii) finally review the prepared structures. Energy minimization was done to clean the steric clashes using Schrodinger restrained minimization (21) in which the heavy atoms are restrained but the output structures do not deviate too much from the input structure. Energy minimization was done using molecular mechanics force field Optimized Potentials for Liquid Simulations (OPLS-2005) (22)**.** The minimization gets completed once the RMSD reaches the cutoff of 0.3Å. The optimization was done to refine the hydrogen atoms. 3D coordinates from the 2D representation of NeuNAc analogue dimers were generated using LigPrep tool of Schrödinger suite (23). For each successfully processed 2D structure, LigPrep generates a single, low-energy, 3D structure with correct chiralities and also produces a number of structures with different ionization states, tautomers, stereochemistries and ring conformations. It also eliminates the unfit molecule through different criteria such as molecular weight and types of functional groups present. Docking investigation was carried out using Glide v5.7 (24)**.** The receptor grid of 20×20×20 $Å^3$ was generated around the binding sites of neuraminidase and haemagglutinin separately using Glide v5.7. Glide applies a sequence of hierarchical filters to search for feasible locations of ligand into the binding site (25). The optimized analogues were flexibly docked in the grid box of the receptor using Monte Carlo based

simulated algorithm (MCSA) minimization. The two docking procedures followed were Glide standard precision (SP) and extra precision (XP). The difference between SP and XP docking is that the SP programs identify the ligands which were responsible for binding and XP docking generates different poses for each successful entered ligand to get a well accurate ranking of least energy models of the complex. The docking pose of each ligand were ranked based on docking score (XPGscore) and docking energy (Glide energies). The ligand with least XPGscore indicates the better binding affinity towards the binding site residues.

Screening of NeuNAc analogues library

The modeled NeuNAc analogues library (Supplement Table 1) was screened against influenza H5N1 neuraminidase and haemagglutinin using Glide standard precision (SP) and extra precision (XP) docking method. Based on the docking score and energy, top five scored NeuNAc analogues complex with each neuraminidase and haemagglutinin were considered for further dimerization Studies. The top five docking score and energy of each Neuraminidase- NeuNAc analogues complex and Haemagglutinin- NeuNAc analogues complex were shown in Table 1.

Modeling of NeuNAc analogue dimers

The following analogues Benzyl-α-5-amino-5d-KDN, 4-Guaniduno-Neu5Ac2en, 4-O-amidinomethyl-Neu5Ac2en, 4-amino-Neu5Ac2en and 5-d-KDN from the top five Neuraminidase- NeuNAc analogues complex and another five analogues KDN, N-glycolyl-NeuNAc, N-crotonoyl-NeuNAc, Neu5Gc and 5-N-thioAc-NeuNAc from the Haemagglutinin- NeuNAc analogues complex were selected for modeling their homo dimers coupled by eight different nano-spacers/linkers using chemical drawing software chemsketch from ACD Labs. The modeled NeuNAc analogue dimers coupled by nano-spacers/linkers were shown in Figure 1.

Molecular dynamics simulation

The Molecular dynamics simulations were carried out for the following complex of influenza neuraminidase – KDN dimer joined by 1-Linker, neuraminidase – KDN dimer attached by CH-C1 nano-spacer and influenza haemagglutinin – KDN dimer connected by CH-C1 nano-spacer and haemagglutinin – KDN dimer coupled by CH-N1 nano-spacer each for 20ns simulation run using Desmond v3.2 software of Schrödinger suite (26). The simulation was carried out to study the stability, conformational change and natural dynamics of the complex in aqueous environment. Desmond is a program designed for explicit solvent simulations i.e., water molecule along with any ions that may present in solvent environment. The force filed computation used in our study is molecular mechanics force field of OPLS-2005 (22). Each complex was solvated using TIP3P water model in an orthorhombic box of suitable size with periodic boundary conditions. The whole system was neutralized by replacing solvent molecules along with adding counter ions Na^+ and Cl^- to balance the net charge of the complex. The whole system of neuraminidase – KDN dimer joined by 1-Linker complex and that is coupled by CH-C1 nano-spacer complex consist of approximately 43,354 and 43,304 atoms respectively. haemagglutinin – KDN dimer linked by CH-C1 nano-spacer complex and that is connected by CH-N1 nano-spacer complex contain 62,092 and 61,883 atoms respectively. The above said complexes were simulated through multistep default protocol formulated in Desmond with a series of restrained minimizations using constant

number of atom (N), pressure (P) and temperature (T) (NPT) ensemble. The system was equilibrated for the simulation time of 12 picoseconds at the temperature of 300 K and pressure at 1.01325 bar. During simulation, each trajectory data frames were collected for every 4.8 ps. Particle-mesh Ewald method were used to compute Long-range electrostatic interactions (27, 28) and Van der waals (VDW) cut off at 9Å. The hydrogen bond geometry constraints were satisfied using SHAKE algorithm (29). The whole system of neuraminidase – KDN dimer joined by 1-Linker as well as coupled by CH-C1 nano-spacer complex, haemagglutinin – KDN dimer linked by CH-C1 nano-spacer as well as connected by CH-N1 nano-spacer complex were analyzed to ascertain their structural stability, dynamics behavior of the complex and their binding nature in water environment using Desmond simulation analysis protocols.

Results and Discussion

Molecular modeling and docking studies of dimers of NeuNAc analogues

To study the fitting of nano-spaced dimers of NeuNAc analogue into the binding sites of H5N1 influenza A viral neuraminidase and haemagglutinin, the following linkers/ nano-spacers having dimensions in nanometer range were chosen for further modeling and simulation studies: 1-Linker of size 2.99nm, CH-C1 nano-spacer of size 2.83nm and CH-N1 nano-spacer of size 2.25nm were used to couple the KDN dimers (Figure 2).

Neuraminidase - NeuNAc analogue dimers complex

In total, eighty NeuNAc analogue dimers (Figure 1) were modeled and docked against the binding sites of H5N1 neuraminidase. The NeuNAc analogue dimers KDN-1-Linker and KDN- CH-C1 Spacer shows favorable interaction towards the binding sites of neuraminidase with docking XPGScores of -15.09 and -15.00 respectively and docking glide energy of -48.63 and -66.93 kcal/mol respectively (Table 2).

Haemagglutinin - NeuNAc analogue dimers complex

Eighty NeuNAc analogue dimers were also screened against the binding site of H5N1 haemagglutinin. The NeuNAc analogue dimers KDN joined by CH-C1 nano-spacer and KDN coupled by CH-N1 nano-spacer show docking score (XPG) of -11.31 and -10.80 respectively and glide docking energy of -56.24 and -50.11 kcal/mol respectively (Table 2).

Molecular dynamics simulation

In current study, the dynamic behavior of NeuNAc analogue dimers fit into the multimeric binding sites of H5N1 neuraminidase - KDN dimer joined by 1-Linker complex, neuraminidase- KDN dimer joined by CH-C1 nano-spacer complex, H5N1 haemagglutinin- KDN dimer joined by CH-C1 nano-spacer complex and haemagglutinin- KDN- CH-N1 Spacer complex were analyzed from the trajectory records acquired from every 20ns MD simulation.

The conformational changes of the complex were checked using Desmond Simulation Quality Analysis and Event Analysis protocol. Past NMR study revealed the benefits of multivalency in which the zanamivir resistant mutants of influenza A virus strains were inhibited by multiple copies of zanamivir conjugated in polymer chain poly-L-glutamine. These multivalent drug varieties demonstrate better viral inhibition due to steric effects and increased affinity (30).

Neuraminidase- KDN dimer joined by 1-Linker complex

The energy transition of the system along with the maintenance of potential energy (E_P), volume, temperature and pressure are shown in Figure 3 (A) during 20 ns simulation run. The essential insight into the protein structural conformation throughout the simulation is recorded as protein – ligand root mean square deviation (RMSD) and Protein RMSD (left Y-axis) is based on the Cα atom selection (Figure 4). The protein RMSD was in the acceptable range of 0.7 – 1.5 Å. Ligand RMSD (right Y-axis) depicts the steady nature of the ligand towards the protein binding sites (Figure 4 (A)). The Root Mean Square Fluctuation (RMSF) is calculated for characterizing local changes in protein side chain. The tails (N- and C-terminal) of the protein fluctuates more than other part of the protein. RMSF of the present protein fluctuates between 0.4 – 2.8 Å (Figure 5 (A)). In an earlier dimeric study, zanamivir dimeric conjugates show pharmacokinetic parameters and neuraminidase inhibitory activity against H5N1 influenza (31).

Interactions of KDN dimer joined by 1-Linker in the binding pocket of neuraminidase were monitored throughout the molecular dynamics simulation of 20ns. Those interactions are depicted as protein – ligand contacts such as hydrogen bonds, hydrophobic, ionic and water bridges (Figure 6 (A)). The hydrogen bond interactions that play major role during the simulations for neuraminidase- KDN dimer joined by 1-Linker complex were calculated for 20000ps. In total, eleven intermolecular hydrogen bonds were found to interact towards the binding site of neuraminidase. The binding site residues GLU277, GLU276, ARG292, ARG371, THR369, SER370, GLU432, and TYR347 were participated in intermolecular hydrogen bonding throughout the trajectory data. The hydrogen atom 85(H) of KDN dimer coupled by 1-Linker formed a hydrogen bond with oxygen atom OE2 of an acidic polar residue GLU277 with a distance of 1.71 Å, the hydrogen atom 84(H) involved in a H-bond with oxygen atom OE2 of acidic polar residue GLU276 with a distance of 1.82 Å, the oxygen atom 98(O) showed a hydrogen bond with HH12 of side chain of basic polar residue ARG292 with a distance of 1.60 Å, the oxygen atom 98(O) participated in a hydrogen bond with HH22 of basic polar side chain residue ARG371 with a distance of 1.58 Å, the oxygen atom 37(O) contributed to a hydrogen bond with HH12 of basic polar side chain residue ARG371 with a distance of 1.71 Å, the hydrogen atom 68(H) showed a H-bond with oxygen atom (O) of polar side chain residue THR369 with a distance of 1.72 Å, the oxygen atom (O) exhibited a H-bond with H of basic polar side chain residue ARG371 with a distance of 2.23 Å, the oxygen atom (O) displayed H-bond with HG of polar side chain residue SER370 with a distance of 1.95 Å, the hydrogen atom 61(H) involved in a H-bond with oxygen atom of acidic polar residues GLU432 with a distance of 1.90 Å, the oxygen atom (O) participated in a H-bond with HH of polar side chain residue TYR347 with a distance of 1.73 and the hydrogen atom 69(H) showed a H-bond with OH of polar side chain residue TYR347 with a distance of 1.95 Å (Figure 7 and Table 3). It was also reported in a previous NMR experimental study concerning the importance of carbohydrate interaction towards the polar amino acid residues (32, 33).

Neuraminidase - KDN dimer coupled by CH-C1 nano-spacer complex

The energy trajectory suggests the steadiness of the complex (Figure 3 (B)) and RMSD of neuraminidase - KDN dimer coupled by CH-C1 nano-spacer complex is as shown in Figure 4(B). Protein RMSD (left Y-axis)

fluctuates between the range of 0.2 – 1.6 Å and ligand RMSD (right Y-axis) indicates that the ligand was fit towards the protein binding sites (Figure 4 (B)). RMSF of present protein chain fluctuates between the range of 0.4 – 2.0 Å (Figure 5 (B)). Protein – ligand contact shows the presence of hydrogen bonds, hydrophobic, ionic and water bridges (Figure 6 (B)). During the simulation, direct intermolecular hydrogen bonds play a major role. Totally, there were nine hydrogen bond interactions with the binding site residues ARG152, GLU119, TYR406, ARG292, ARG371 and TYR347.

Fig.1 The structure and abbreviation of NeuNAc analogues coupled with different Linkers/Nano-Spacers of length in nm

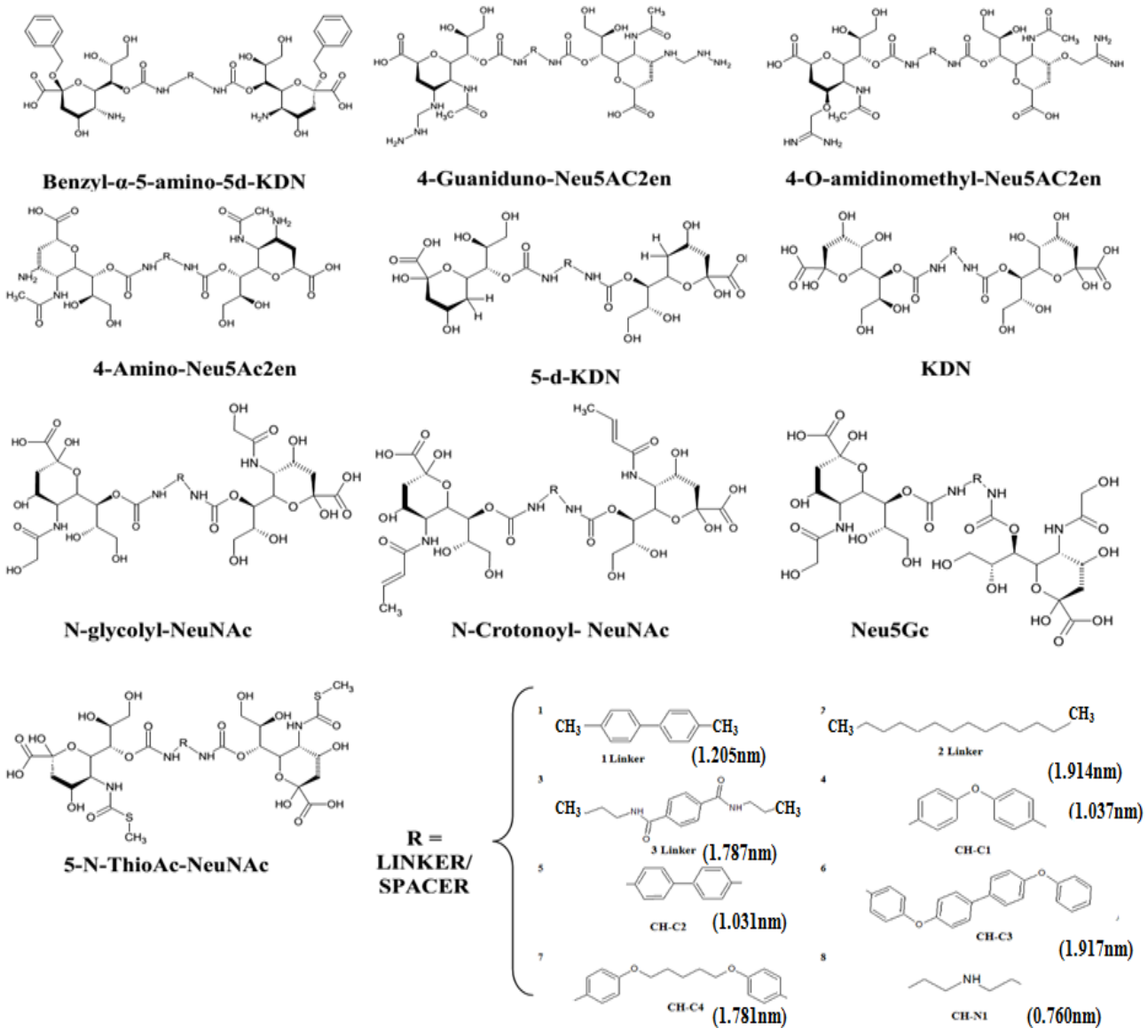

Fig.2 The NeuNAc analogue dimers of KDN joined by 1-Linker, KDN connected by CH-C1 nano-spacer and KDN linked by CH-N1 nano-spacer

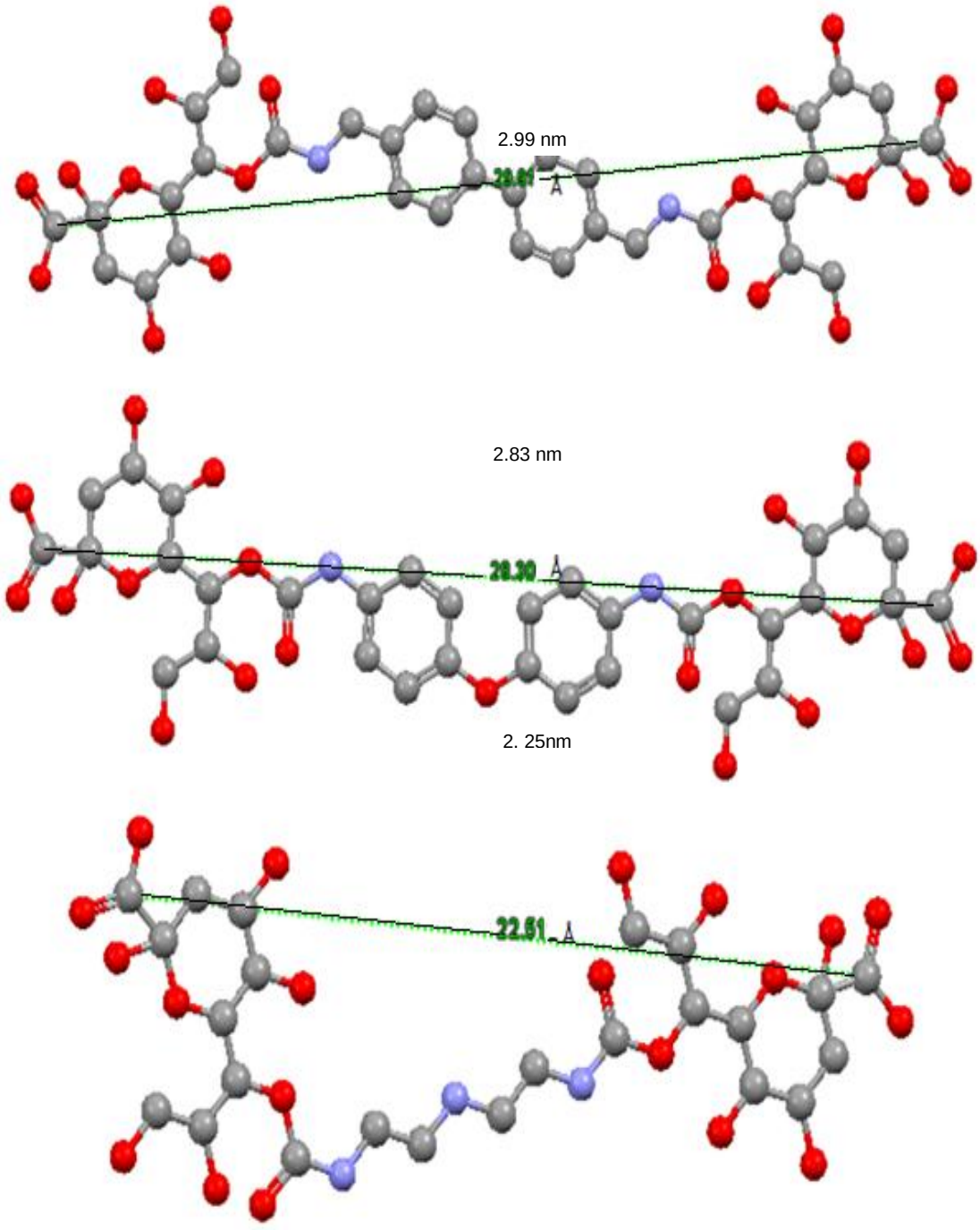

Fig.3 Energy diagram of (A) Neuraminidase - KDN dimer joined by 1-Linker complex, (B) Neuraminidase - KDN dimer coupled by CH-C1 nano-spacer complex, (C) Haemagglutinin - KDN dimer coupled by CH-C1 nano-spacer complex and (D) Haemagglutinin - KDN dimer connected by CH-N1 nano-spacer complex for each 20ns respectively

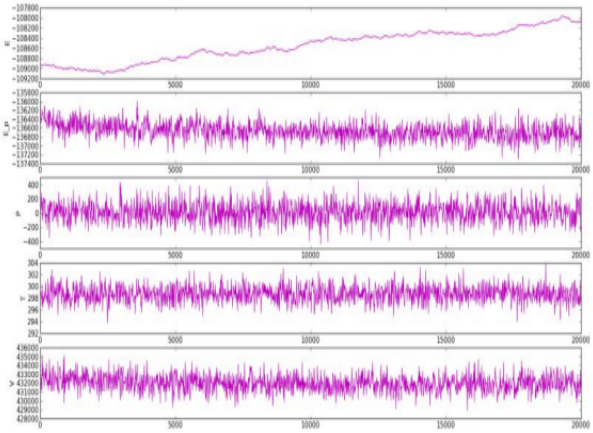

(A) Neuraminidase - KDN-1-Linker complex

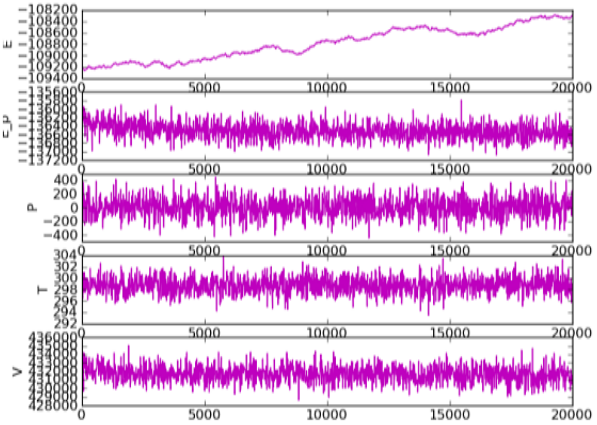

(B) Neuraminidase - KDN-CH-C1 Spacer complex

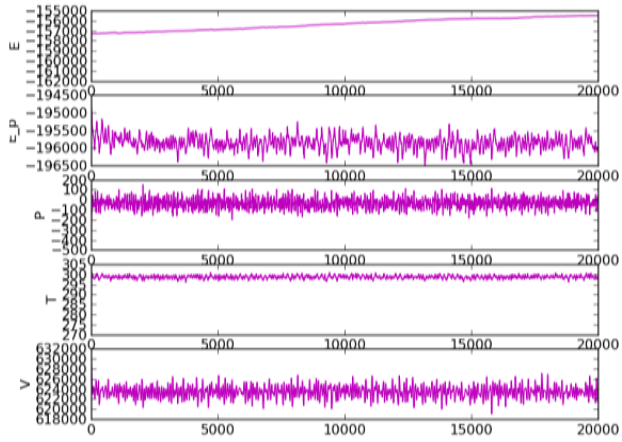

(C) Haemagglutinin - KDN-CH-C1 Spacer complex

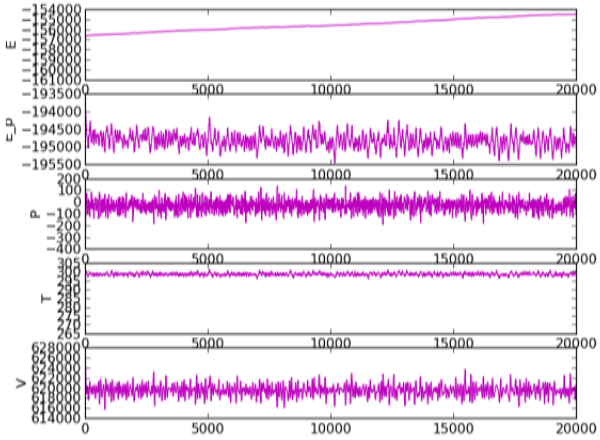

(D) Haemagglutinin - KDN-CH-N1 Spacer

Fig.4 Protein – Ligand RMSD of (A) Neuraminidase - KDN dimer joined by 1-Linker complex, (B) Neuraminidase - KDN dimer coupled by CH-C1 nano-spacer complex, (C) Haemagglutinin - KDN dimer coupled by CH-C1 nano-spacer complex and (D) Haemagglutinin - KDN dimer connected by CH-N1 nano-spacer complex for each 20ns respectively

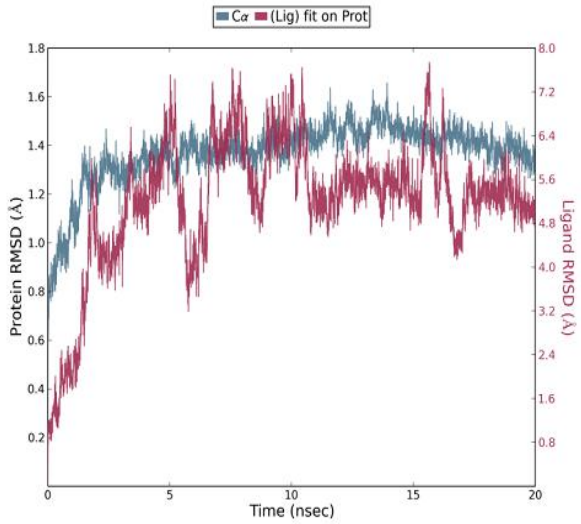

(A) Neuraminidase - KDN-1-Linker

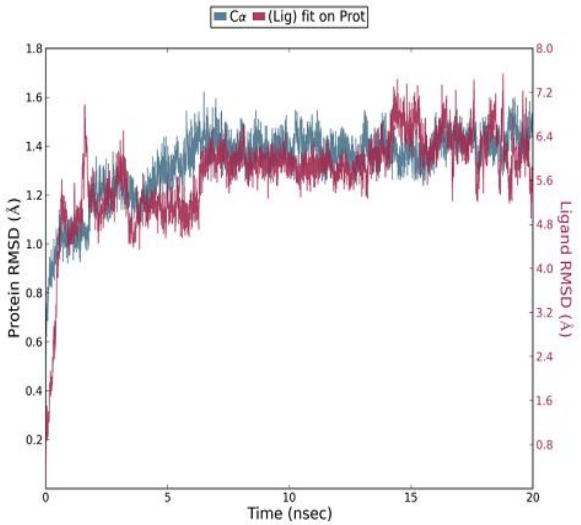

(B) Neuraminidase - KDN-CH-C1 Spacer complex

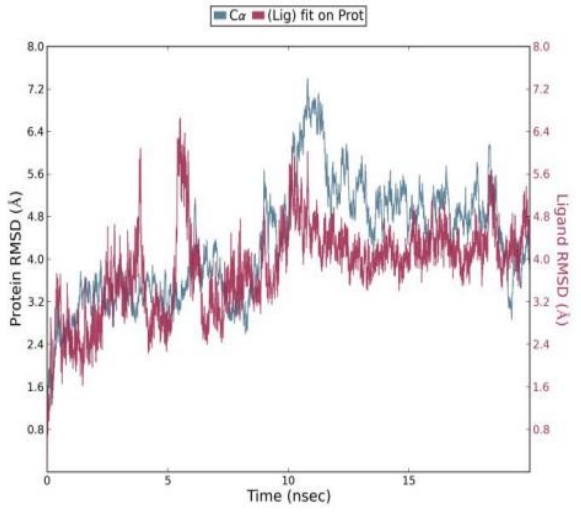

(C) Haemagglutinin- KDN- CH-C1 Spacer complex

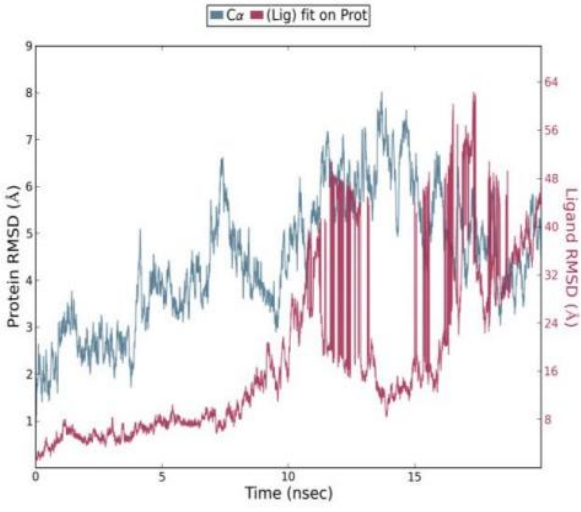

(D) Haemagglutinin- KDN- CH-N1 Spacer complex

Fig.5 RMSF of (A) Neuraminidase - KDN dimer joined by 1-Linker complex, (B) Neuraminidase - KDN dimer coupled by CH-C1 nano-spacer complex, (C) Haemagglutinin - KDN dimer coupled by CH-C1 nano-spacer complex and (D) Haemagglutinin - KDN dimer connected by CH-N1 nano-spacer complex for each 20ns respectively

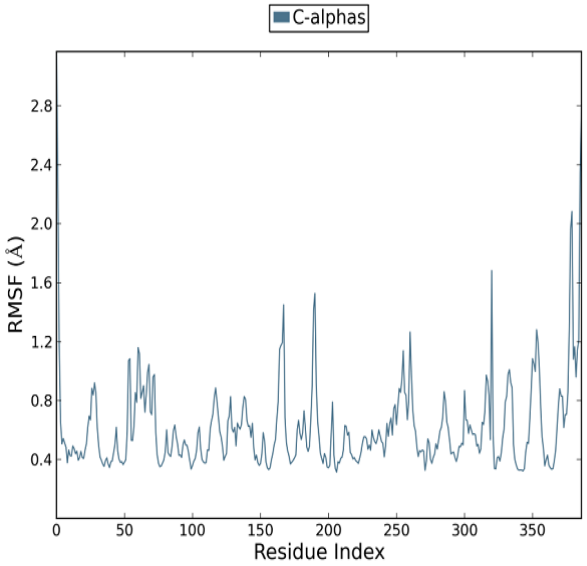

(A) Neuraminidase - KDN-1-Linker complex

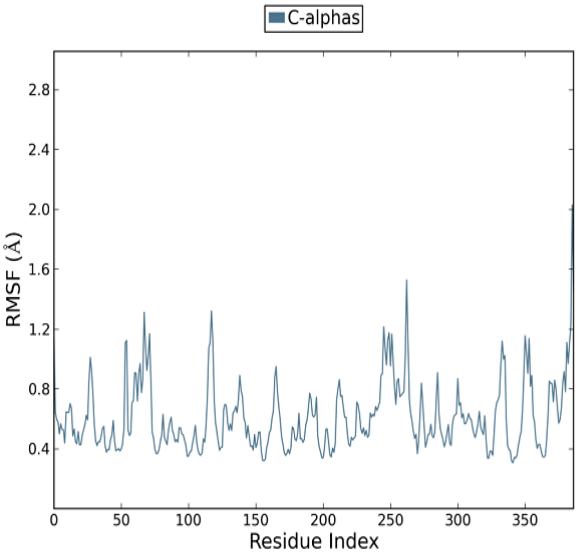

(B) Neuraminidase - KDN-CH-C1 Spacer

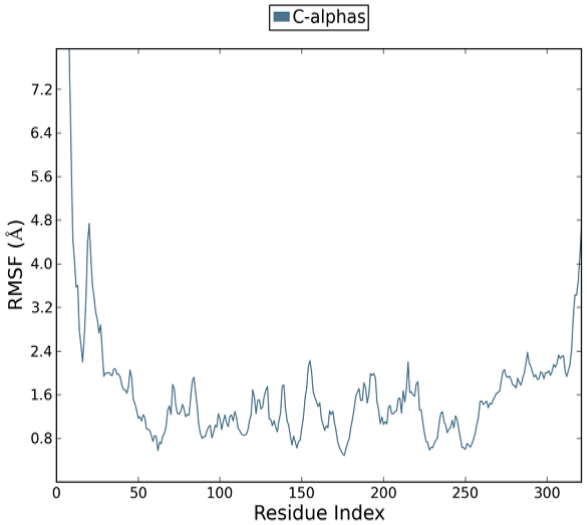

(C) Haemagglutinin - KDN-CH-C1 Spacer complex

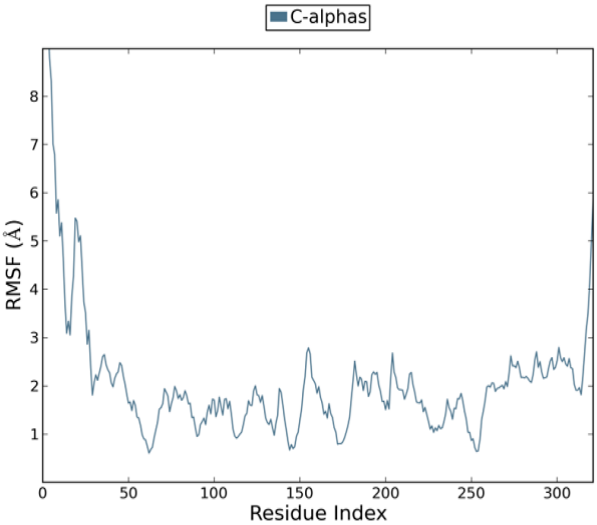

(D) Haemagglutinin - KDN-CH-N1 Spacer complex

Fig.6 Protein – Ligand contact of (A) Neuraminidase - KDN dimer joined by 1-Linker complex, (B) Neuraminidase - KDN dimer coupled by CH-C1 nano-spacer complex, (C) Haemagglutinin - KDN dimer coupled by CH-C1 nano-spacer complex and (D) Haemagglutinin - KDN dimer connected by CH-N1 nano-spacer complex for each 20ns respectively

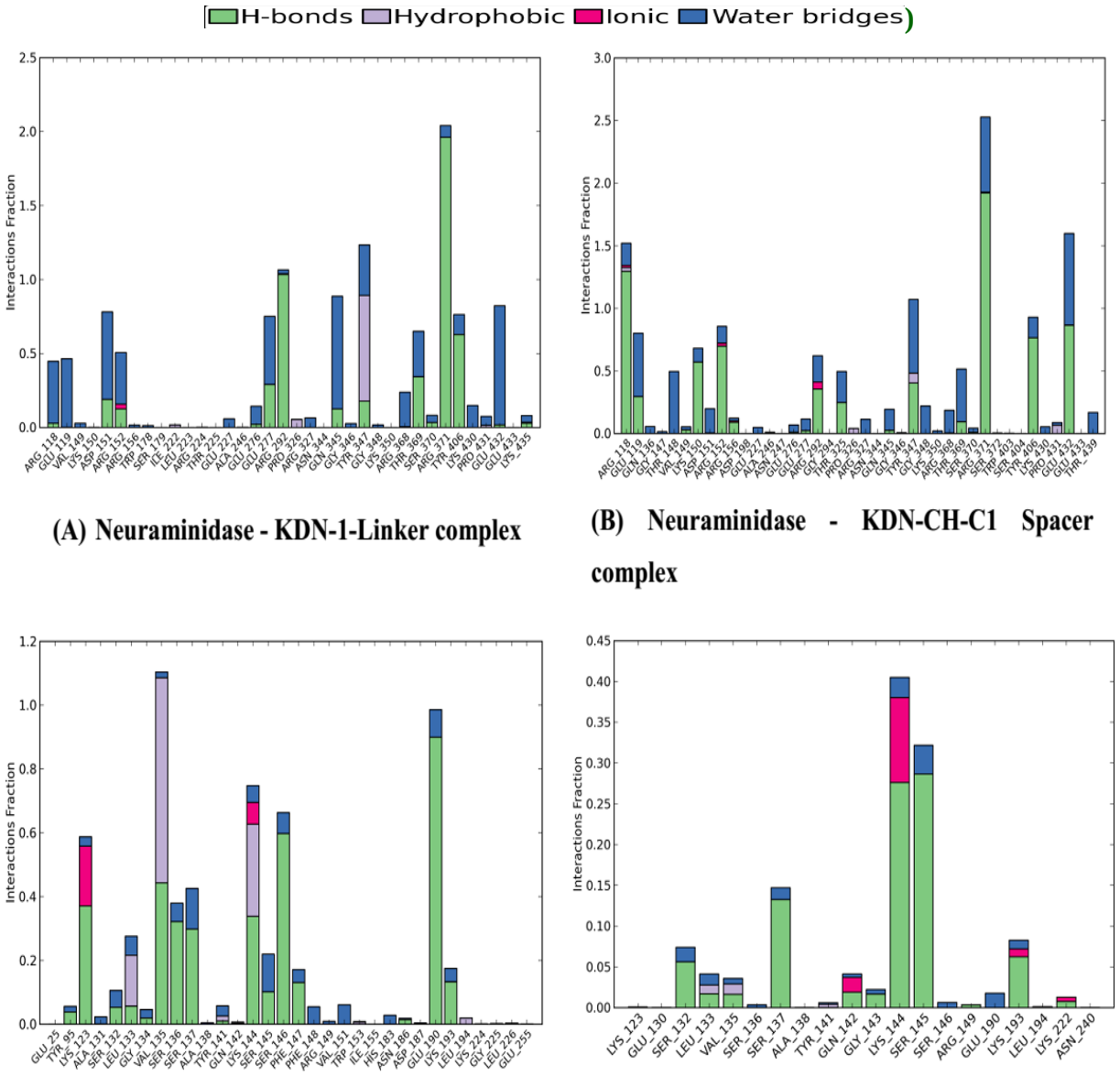

(A) Neuraminidase - KDN-1-Linker complex

(B) Neuraminidase - KDN-CH-C1 Spacer complex

(C) Haemagglutinin - KDN-CH-C1 Spacer complex

(D) Haemagglutinin - KDN-CH-N1 Spacer complex

Fig.7 A: 3D render of Neuraminidase bound with KDN dimer joined by 1-Linker complex and B: Intermolecular hydrogen bonding of the complex for 20 ns simulation run (Note: → H-bond back bone; ⇢ H-Bond side chain; → water bridge)

A:

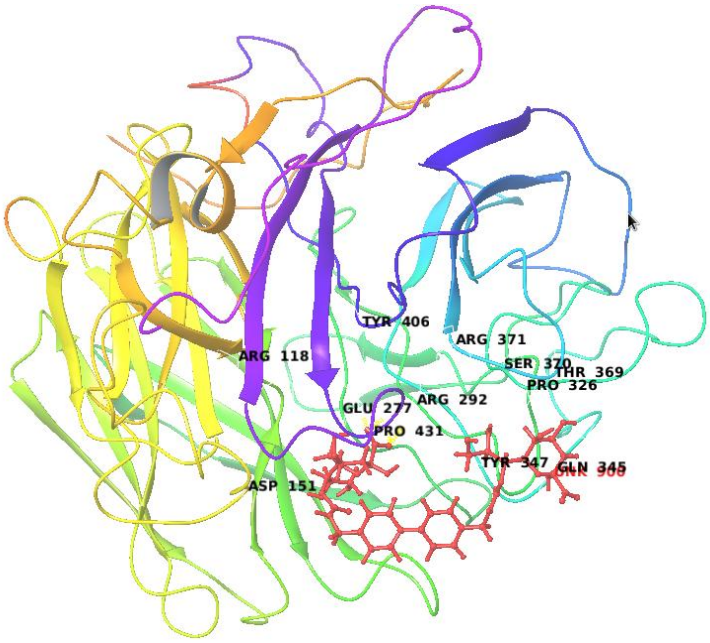

B:

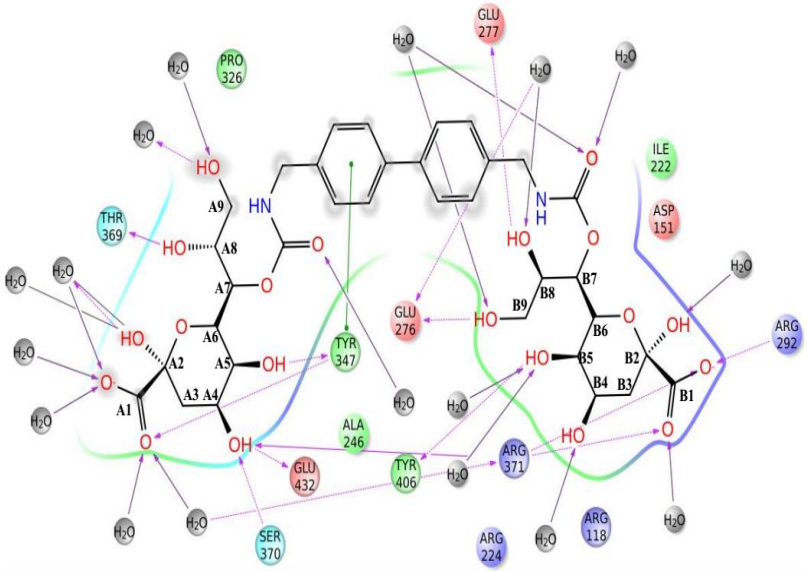

Neuraminidase - KDN-1-Linker complex

Fig.8 A: 3D render of Neuraminidase bound with KDN dimer coupled by CH-C1 nano-spacer complex and B: Intermolecular hydrogen bonding of the complex for 20 ns simulation run (Note: → H-bond back bone; ⇢ H-Bond side chain; → water bridge)

A:

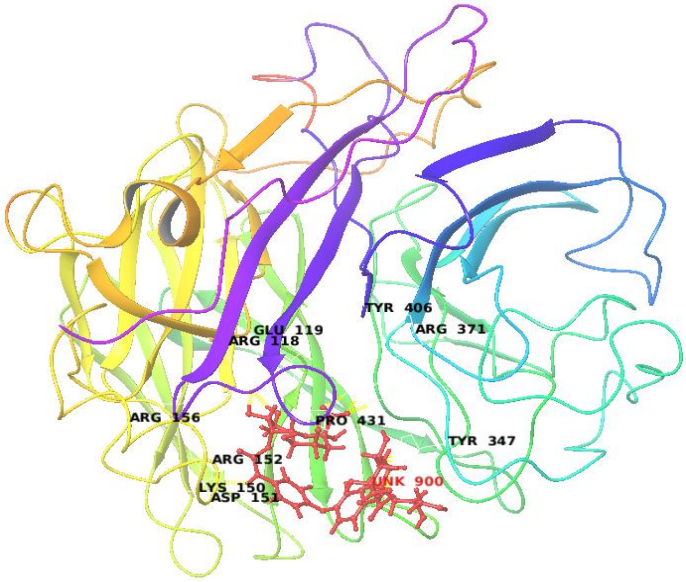

B:

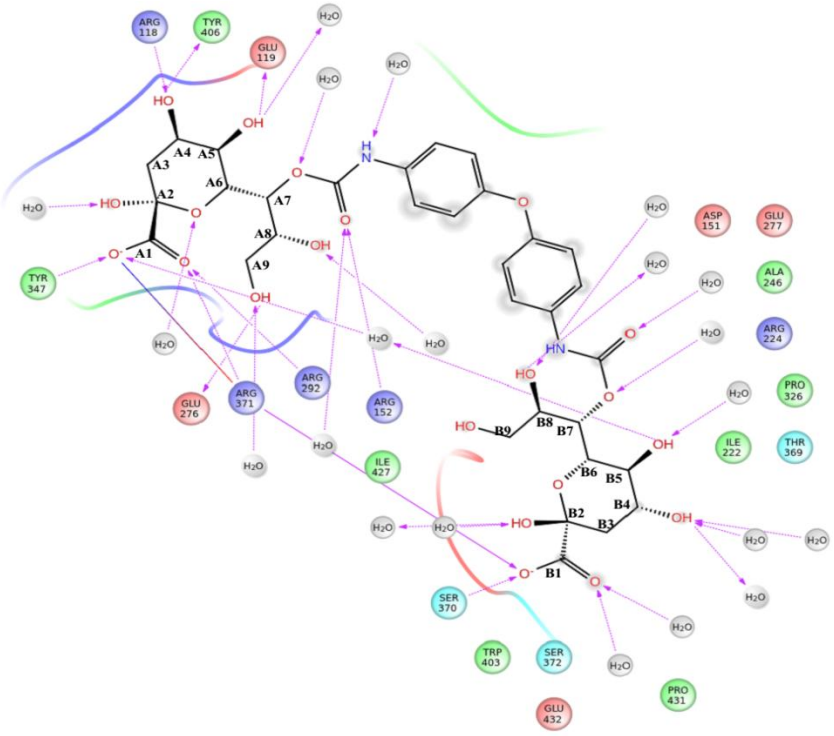

Neuraminidase - KDN-CH-C1 Spacer complex

Fig.9 A: 3D render of Haemagglutinin bound with KDN dimer coupled by CH-C1 nano-spacer complex and B: Intermolecular hydrogen bonding of the complex for 20 ns simulation run (Note: → H-bond back bone; ⇢ H-Bond side chain; → water bridge)

A:

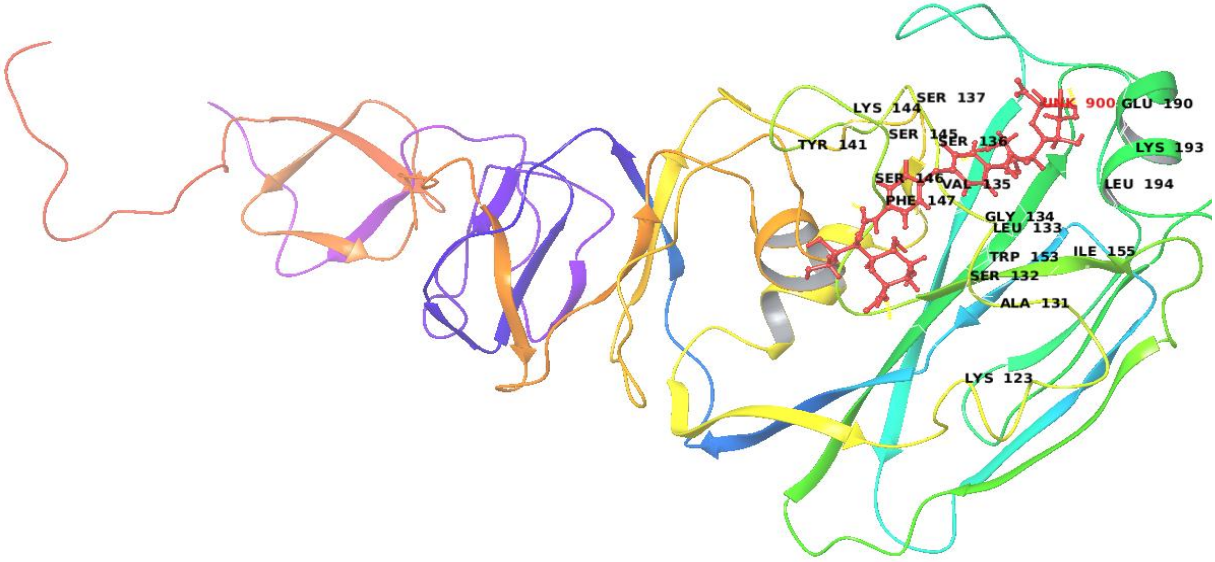

B:

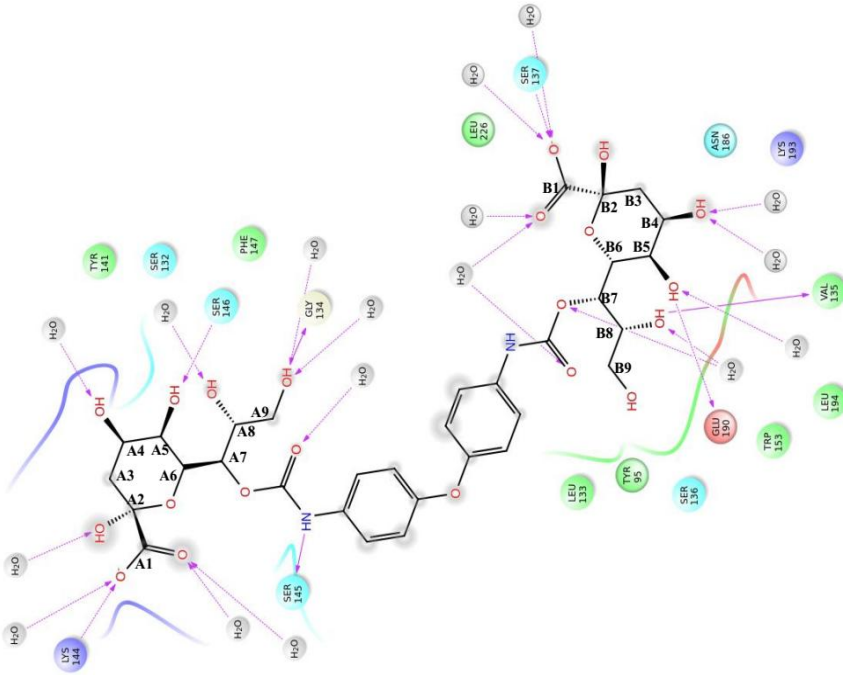

Haemagglutinin - KDN-CH-C1 Spacer complex

Fig.10 A: 3D render of Haemagglutinin bound with KDN dimer connected by CH-N1 nano-spacer complex and B: Intermolecular hydrogen bonding of the complex for 20 ns simulation run (Note: → H-bond back bone; ⇢ H-Bond side chain; → water bridge)

A:

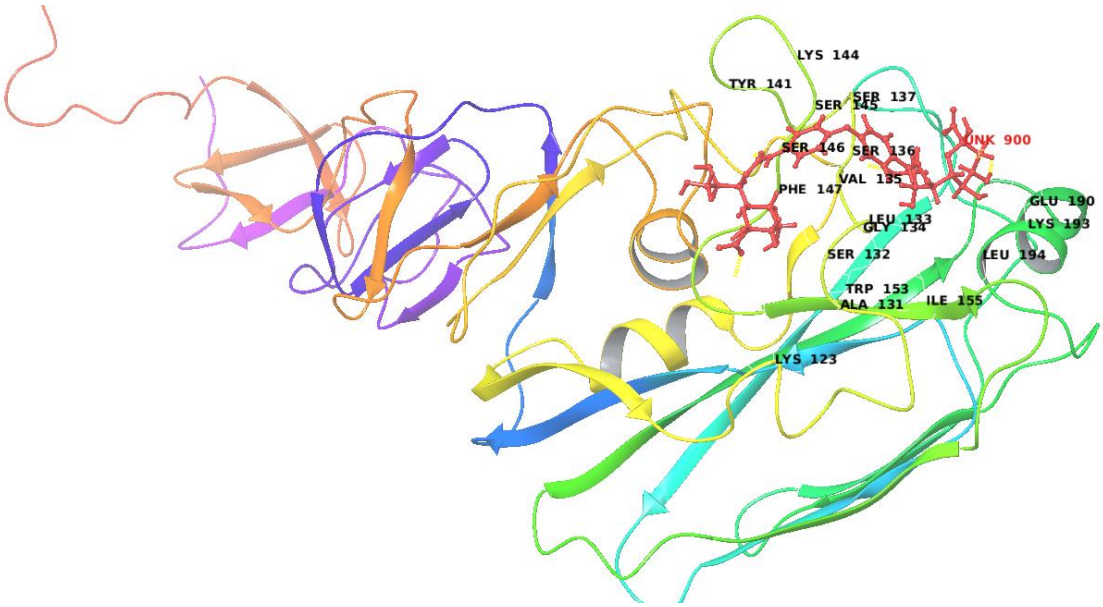

B:

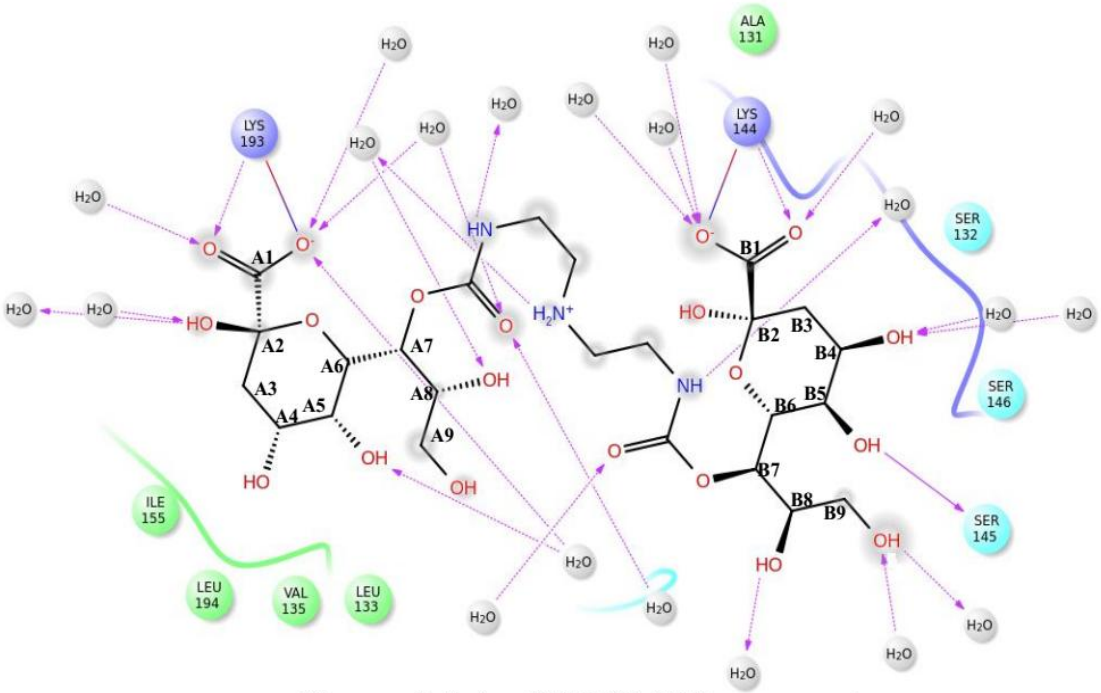

Haemagglutinin - KDN-CH-N1 Spacer complex

Fig.11 Ligand Torsion Profile for Neuraminidase - KDN dimer joined by 1-Linker complex for 20 ns simulation run

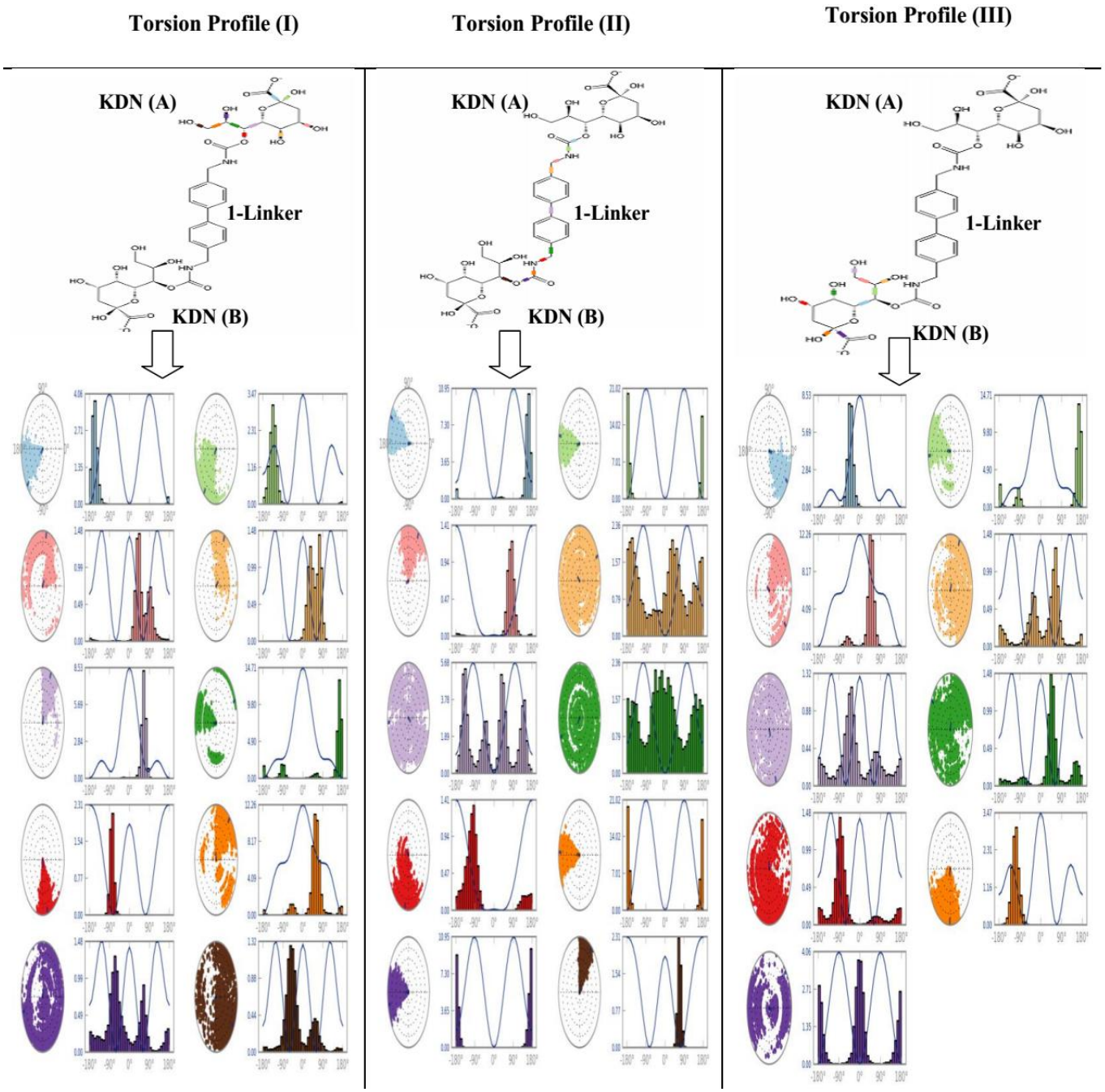

Fig.12 Ligand Torsion Profile for Neuraminidase - KDN dimer coupled by CH-C1 nano-spacer complex for 20 ns simulation run

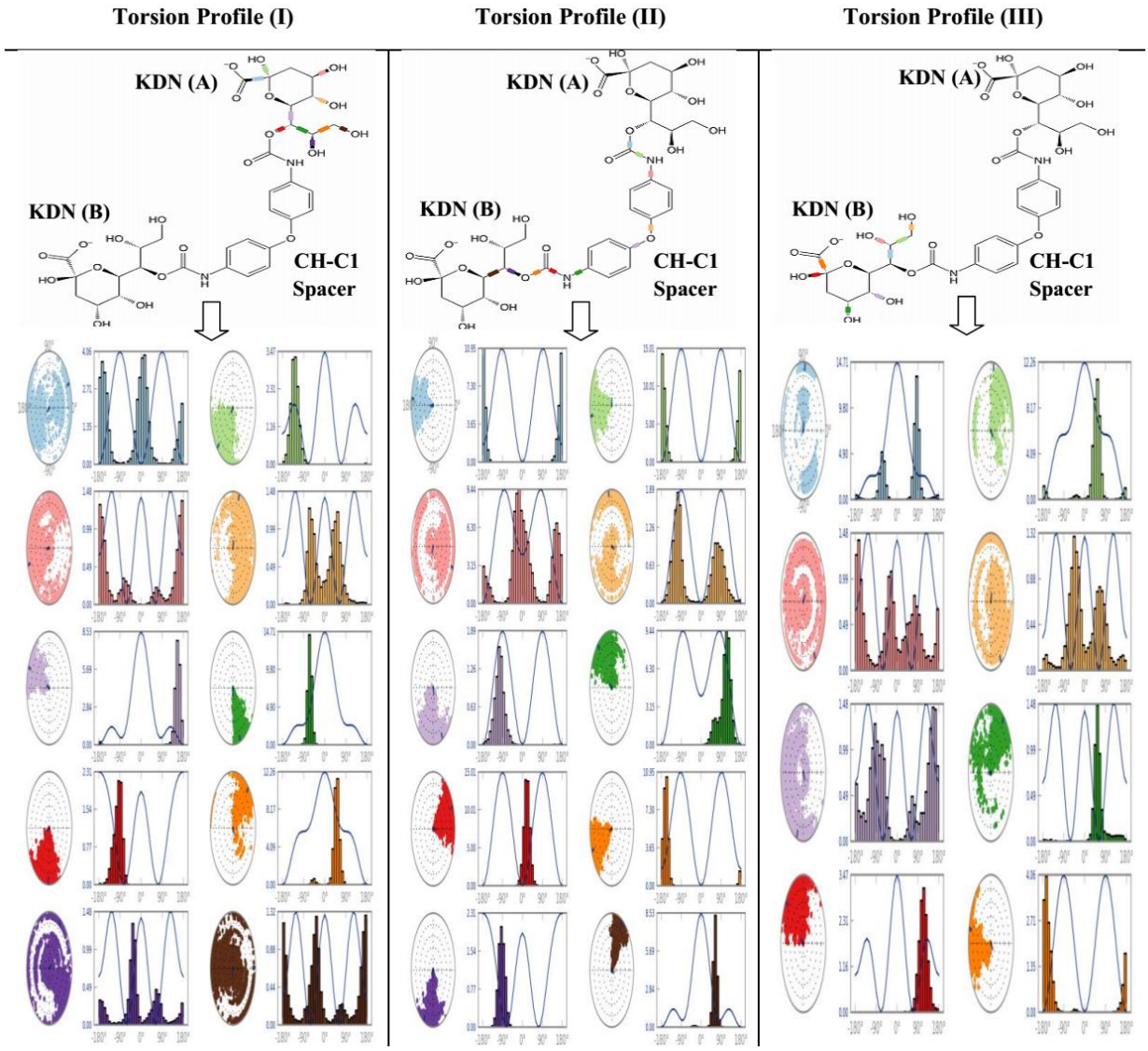

Fig.13 Ligand Torsion Profile for Haemagglutinin - KDN dimer coupled by CH-C1 nano-spacer complex for 20ns simulation run

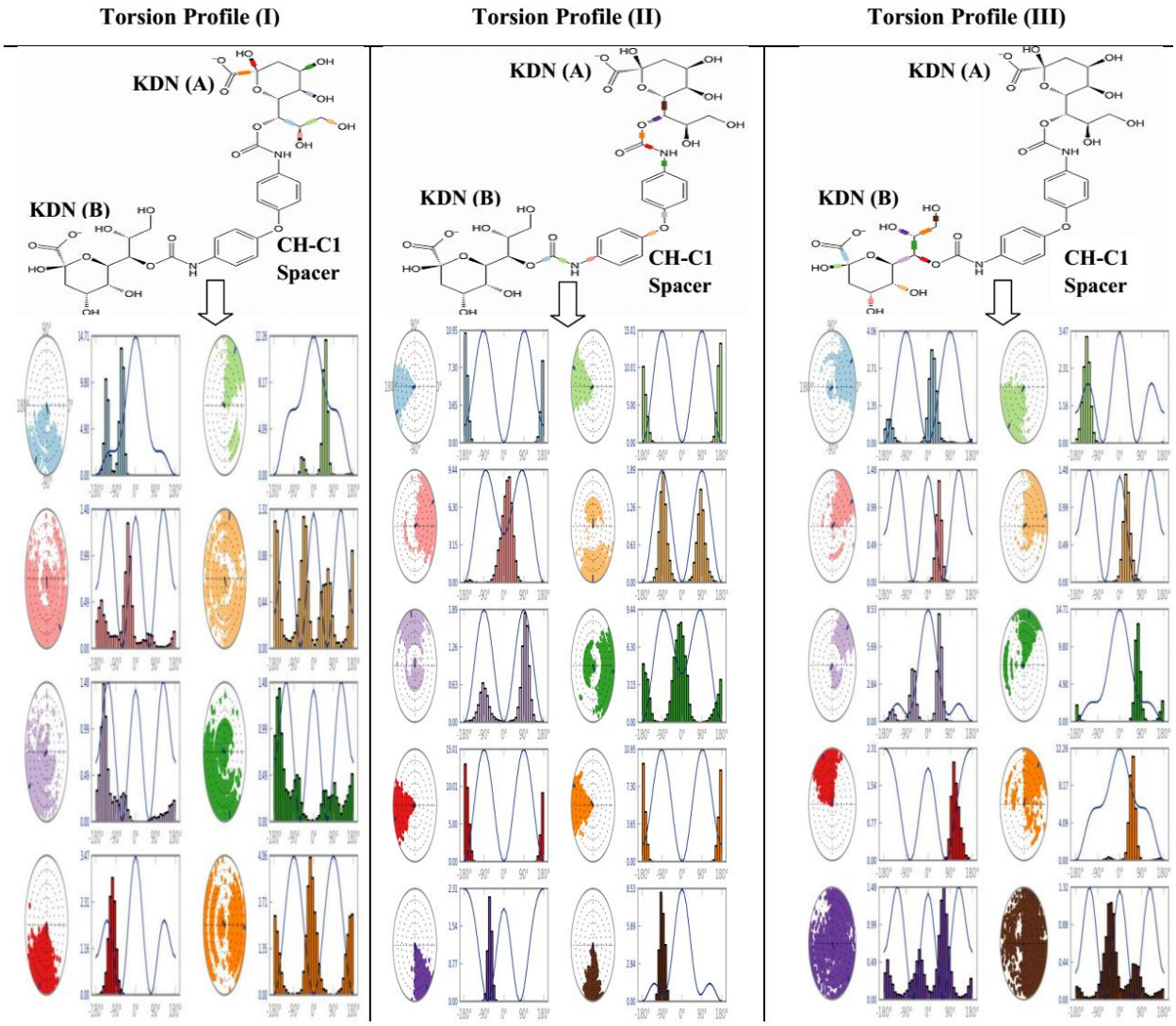

Fig.14 Ligand Torsion Profile for Haemagglutinin - KDN dimer connected by CH-N1 nano-spacer complex for 20 ns simulation run

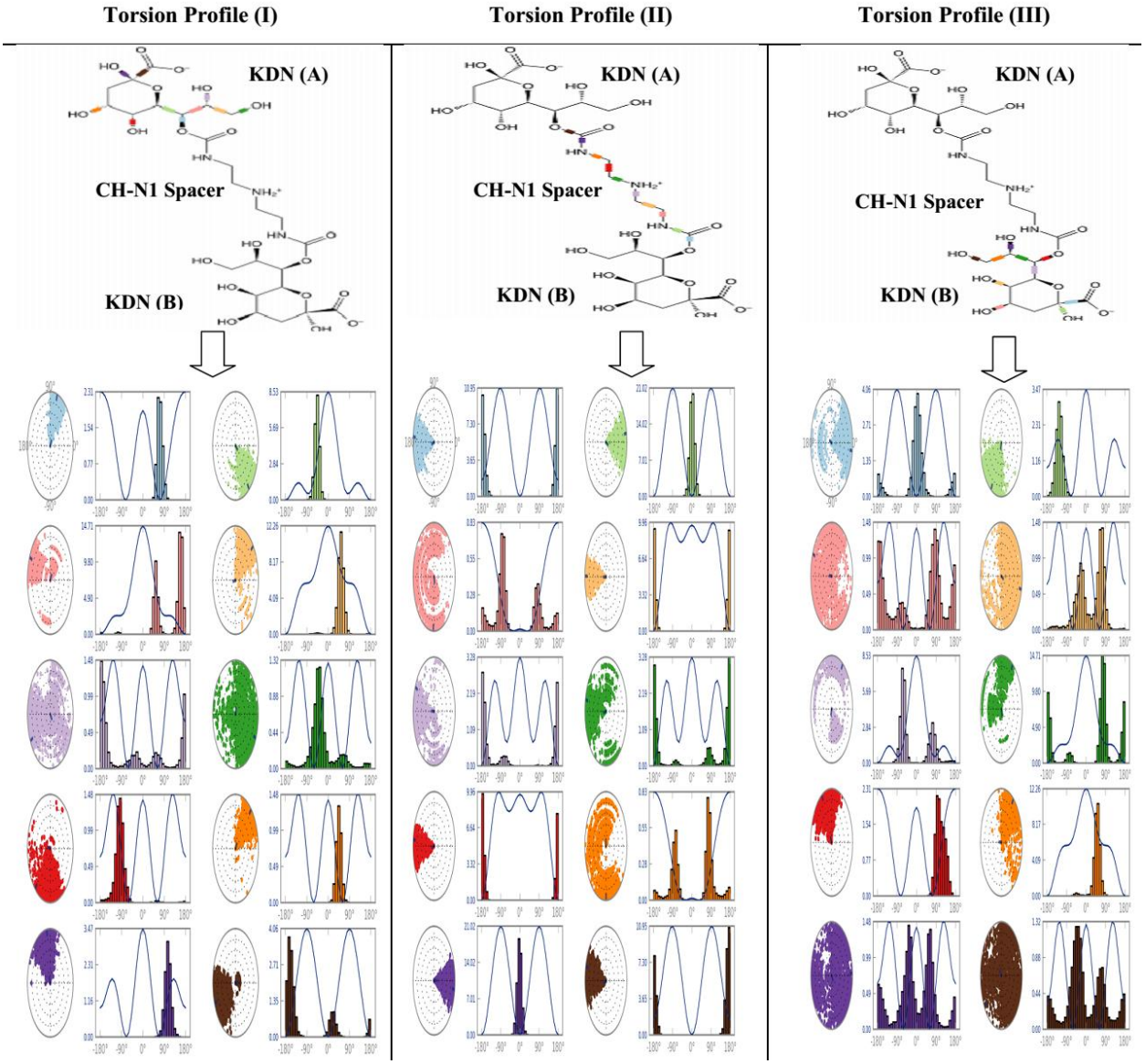

Table.1 Glide dock score, Glide dock energy and inter molecular hydrogen bond interaction of NeuNAc analogue monomer complex with influenza H5N1 viral proteins neuraminidase and haemagglutinin

H5N1 Neuraminidase							
Sl.No	**NeuNAc Analogues**	**Glide Docking Score**	**Glide Docking Energy kcal/mol**	**Neuraminidase Protein**		**Ligand Atom**	**Distance (Å)**
				Residues	**Atoms**		
1	Benxyl-α-5-amino-5d-KDN	-12.65	-37.61	GLU:119 ARG:118 TRY:406 ARG:371 TYR:347 ARG:292 ARG:292 GLU:277 GLU:276	OE2 HH22 OH HH22 HH HH12 HH22 OE2 OE2	38 (H) O 30 (H) 23 (O) 15 (O) 48 (O) 48 (O) 36 (H) 37 (H)	2.281 1.871 1.605 1.918 2.004 1.926 1.853 1.776 1.693
2	4-Guaniduno-Neu5Ac2en	-12.52	-55.25	ARG:118 ARG:371 GLU:119 GLU:277 ARG:371 ARG:292 ALA:246 ARG:152	HH22 HH22 OE2 OE2 HH12 HH22 O HH22	8 (O) 8 (O) 48 (H) 45 (H) 47 (O) 47 (O) 34 (H) 19 (O)	2.396 2.130 2.360 2.145 1.600 2.134 2.169 1.946
3	4-O-amidinomethyl-Neu5Ac2en	-12.15	-40.42	ARG:371 ARG:371 ARG:292 ARG:292 GLU:277 GLU:277 GLU:277 ASP:151 ARG:152 ARG:152	HH22 HH12 HH22 HH12 OE2 OE2 OE2 OD2 HH22 HH22	O O 46 (O) 46 (O) 44 (H) 43 (H) 45 (H) 34 (H) 14 (O) 13 (O)	2.308 2.141 1.993 1.831 2.050 1.631 2.185 1.936 2.434 2.083
4	4-Amino-Neu5Ac2en	-12.13	-45.45	GLU:119 ASP:151 ARG:152 ASP:151 ARG:152 ARG:371 TYR:347	OE2 OD1 HH21 OD2 HH22 HH12 HH	26 (H) 41 (H) 19 (O) 33 (H) 13 (O) 8 (O) 40 (O)	1.732 2.049 1.990 2.008 1.960 1.683 1.930
5	5-d-Kdn	-11.87	-26.93	GLU:227 GLU:277 TYR:406	OE2 OE2 OH	29 (H) 31 (H) 23 (H)	1.924 1.901 1.802

				ARG:292 ARG:371 ARG:371 ARG:292 TYR:347 ARG:118	HH22 HH22 HH12 HH12 HH HH22	32 (H) O O 32 (O) O O	1.897 2.172 1.738 1.679 2.329 1.707
H5N1 Haemagglutinin							
Sl.No	**NeuNAc Analogues**	**Glide Docking Score**	**Glide Docking Energy kcal/mol**	**Haemagglutinin Protein**		**Ligand Atom**	**Distance (Å)**
				Residues	**Atoms**		
1	KDN	-8.97	-34.8	LYS:193 GLU:190 SER:136 VAL:135 LEU:133 SER:137	HZ3 OE2 HG O O OG	O 25 (H) O 24 (H) 23 (H) 30 (H)	1.730 2.283 2.163 2.199 1.979 1.923
2	N-Glycolyl-NeuNAc	-8.45	-40.37	GLU:190 LEU:133 VAL:135 SER:136 SER:136 SER:137	OE2 O O HG HG OG	27 (H) 34 (H) 33 (H) O O 39 (H)	1.982 1.933 1.715 2.194 2.304 1.853
3	N-Crotonoyl-NeuNAc	-8.38	-39.77	LEU:133 VAL:135 SER:136 SER:137 GLU:190 LYS:193	O O HG OG OE2 HZ3	28 (H) 37 (H) O 34 (H) 29 (H) O	2.175 1.918 2.291 1.977 2.119 1.712
4	Neu5Gc	-8.23	-38.80	LEU:133 VAL:135 SER:136 SER:137 LYS:193	O O HG OG HZ3	35 (H) 34 (H) O 39 (H) O	2.074 1.827 2.362 2.008 1.646
5	5-N-thioAc-NeuNAc	-8.20	-39.24	LEU:133 VAL:135 SER:136 SER:137 GLU:190 LYS:193	O O HG OG OE2 HZ3	27 (H) 34 (H) O 33 (H) 28 (H) 40 (O)	2.060 2.071 2.304 1.933 2.270 1.709
6	Co-crystal NAG_SIA	-5.26	-31.16	GLU:190 SER:137 SER:136 LEU:133	OE2 H HG O	H40 O12 O12 H58	2.350 2.070 2.129 1.919

Table.2 Enhanced Glide dock score, Glide dock energy and inter molecular hydrogen bond interaction of dimers of NeuNAc analogues complex with influenza H5N1 Neuraminidase and influenza H5N1 Haemagglutinin viral proteins

H5N1 Neuraminidase							
Sl.No	**NeuNAc Analogues**	**Glide Docking Score**	**Glide Docking Energy kcal/mol**	**Neuraminidase Protein**		**Ligand Atom**	**Distance (Å)**
				Residues	**Atoms**		
1	KDN-1-Linker	-15.09	-48.63	GLU:432 ARG:371 THR:369 THR:369 ARG:371 ARG:371 TYR:347 ARG:292 ARG:292 GLU:119	OE1 H O O HH22 HH12 HH HH12 HH22 OE2	61 (H) O 69 (H) 68 (H) 98 (O) 98 (O) 29 (O) 37 (O) 37 (O) 87 (H)	2.112 1.957 2.261 2.047 2.034 1.720 2.032 1.826 1.872 1.832
2	KDN-CH-C1 Spacer	-15.00	-66.93	GLU:432 ARG:371 TYR:347 ARG:371 ARG:118 TYR:406 GLU:119 ARG:292 GLU:276	OE1 H OH HH12 HH22 OH OE2 HH12 OE2	61 (H) 94 (O) 60 (H) 93 (O) 33 (O) 79 (H) 88 (H) 42 (O) 85 (H)	1.895 2.099 2.137 1.796 1.616 1.816 1.744 1.673 1.732
3	Zanamivir	-9.10	-39.23	ARG:152 TRP:178 TRP:178 ASP:151 ASP:151 ARG:118 ARG:371 TYR:347 GLU:276	O H38 H40 H39 H43 O42 O42 O6 H37	HH21 O O O OD1 HH22 HH22 HH OE2	1.988 1.728 2.167 1.893 2.298 1.767 1.951 2.024 1.971
H5N1 Haemagglutinin							
Sl.No	**NeuNAc Analogue dimers at sialic acid binding site**	**Glide Docking Score**	**Glide Docking Energy kcal/mol**	**Haemagglutinin Protein**		**Ligand Atom**	**Distance (Å)**
				Residues	**Atoms**		
1	KDN-CH-C1 Spacer	-11.31	-56.24	GLU:190 GLU:190 SER:137	OE2 OE2 H	68 (H) 60 (H) 94 (O)	1.832 1.950 2.152

				VAL:135 LEU:133 SER:145 SER:146 LYS:144	O O O HG HZ2	66 (H) 67 (H) 89 (H) 38 (O) 93 (O)	1.700 2.066 2.009 2.224 1.775
2	KDN-CH-N1 Spacer	-10.80	-50.11	LYS:114 LYS:114 SER:145 SER:145 SER:132 VAL:135 LEU:133 LEU:133 LYS:193	HZ3 HZ2 O O O O O O HZ3	41 (O) 87 (O) 83 (H) 85 (H) 87 (H) 59 (H) 60 (H) 52 (H) O	2.181 2.291 1.754 1.824 2.276 2.081 2.495 2.143 1.903
Sl.No	**NeuNAc Analogue dimers at different binding sites**	**Glide Docking Score**	**Glide Docking Energy kcal/mol**	**Haemagglutinin Protein**		**Ligand Atom**	**Distance (Å)**
				Residues	**Atoms**		
1	KDN-1-Linker-dimer	-9.48	-47.36	ASN:88 ALA:87 LYS:70 LYS:106 ILE:268 GLU:104	OD1 O HZ1 HZ1 H OE2	H84 H85 37O 98O O H70	2.150 1.773 1.809 1.912 1.973 1.998
2	5-d-KDN-CH-N1-Spacer-dimer	-8.27	-50.28	HIS:107 THR:267 GLU:103 ILE:268 LYS:106 LYS:270 ALA:87	NE2 HG1 OE2 O HZ1 HZ1 O	H54 O16 H86 H61 O41 O85 H83	2.357 2.001 1.717 2.373 1.844 1.724 1.748
3	KDN-CH-N1-Spacer-Dimer	-8.02	-49.24	THR:267 GLU:103 LYS:106	HG1 O HZ1	O17 H58 O32	1.890 1.765 1.919
4	5-d-KDN-CH-C1-Spacer Dimer	-6.73	-47.40	GLU:104 GLU:103 GLU:103 LYS:106 LYS:270	OE2 O OE2 HZ1 HZ1	H90 H88 H70 O29 O	2.425 1.926 1.694 1.977 1.799

Table.3 Inter molecular hydrogen bond distance for dimers of NeuNAc analogues: Neuraminidase - KDN dimer joined by 1-Linker complex, Neuraminidase - KDN dimer coupled by CH-C1 nano-spacer complex, Haemagglutinin - KDN dimer coupled by CH-C1 nano-spacer complex and Haemagglutinin - KDN dimer connected by CH-N1 nano-spacer complex each 20ns respectively

H5N1 Neuraminidase							
Sl.No	**Dimer Neu5Ac analogues**	**MD simulation**	**Total NO. of interaction**	**Protein**		**Ligand Atoms**	**Distance Å**
				Residues	**Atoms**		
1	KDN-1-Linker	20ns	11	GLU:277 GLU:276 ARG:292 ARG:371 ARG:371 THR:369 ARG:371 SER:370 GLU:432 TYR:347 TYR:347	OE2 OE2 HH12 HH22 HH12 O H HG OE1 HH OH	85 (H) 84 (H) 98 (O) 98 (O) 37 (O) 68 (H) O O 61 (H) O 69 (H)	1.71 1.82 1.60 1.58 1.71 1.72 2.23 1.95 1.90 1.73 1.95
2	KDN-CH-C1 Spacer	20ns	9	ARG:152 GLU:119 TYR:406 ARG:292 ARG:371 TYR:347 TYR:347 ARG:371 ARG:371	HH12 OE1 OH HH12 HH12 HH OH H HH22	40 (O) 88 (H) 79 (H) 42 (O) 42 (O) 93 (O) 67 (O) O 33 (O)	2.20 1.97 1.97 1.60 1.63 1.82 1.89 1.85 2.44
H5N1 Haemagglutinin							
Sl.No	**Dimer Neu5Ac analogues**	**MD simulation (ns)**	**Total NO. of interaction**	**Protein**		**Ligand Atoms**	**Distance Å**
				Residues	**Atoms**		
1	KDN-CH-C1 Spacer	20ns	7	GLU:190 SER:137 VAL:135 SER:145 GLY:134 LYS:144 SER:146	OE2 HG O O O HZ1 HG	68 (H) 94 (O) 67 (H) 89 (H) 85 (H) 93 (O) 44 (O)	1.80 2.05 1.83 1.96 1.90 1.65 2.16
2	KDN-CH-N1 Spacer	20ns	4	LYS:144 SER:145 LYS:193 LEU:133	HZ1 O HZ3 O	41 (O) 85 (H) O 52 (H)	1.66 2.52 2.03 1.95

The oxygen atom 40(O) formed a hydrogen bond with HH12 of basic polar side chain residue ARG152 with a distance of 2.20 Å, the hydrogen atom 88(H) showed a H-bond with oxygen atom OE1 of acidic polar residue GLU119 with a distance of 1.97 Å, the hydrogen atom 79(H) displayed a H-bond with OH of polar side chain residue TYR406 with a distance of 1.97 Å, the oxygen atom 42(O) showed a H-bond with HH12 of basic polar side chain residue ARG292 with a distance of 1.60 Å, another hydrogen bond with HH12 of basic polar side chain residue ARG371 with a distance of 1.63 Å, the oxygen atom 93(O) participated in a H-bond with HH of polar side chain residue TYR347 with a distance of 1.82 Å, the oxygen atom 67(O) exhibited a H-bond with OH of polar side chain residue TYR347 with a distance of 1.89 Å, the oxygen atom (O) formed a H-bond with H of basic polar side chain residue ARG371 with a distance of 1.85 Å and the oxygen atom 33(O) showed a H-bond with HH22 of basic polar side chain residue ARG371 with a distance of 2.44 Å (Figure 8 and Table 3). A previous NMR spectroscopy report records the inhibition of active site residues of rhesus rotavirus hemagglutinin by sialic acid responsible for host specificity (34).

Haemagglutinin - KDN dimer coupled by CH-C1 nano-spacer complex

The energy curve illustrates the steady nature of the complex (Figure 3 (C)). The MD simulation of haemagglutinin - KDN dimer coupled by CH-C1 nano-spacer complex shows optimal binding interaction. The whole system was observed steady as illustrated using RMSD, RMSF, Protein – ligand contacts. The RMSD of Haemagglutinin - KDN dimer coupled by CH-C1 nano-spacer complex fluctuates between the range of 0.8 – 5.6 Å (Figure 4 (C)). RMSF of the protein side chain fluctuates between the range of 0.8 – 2.4 Å (Figure 5 (C)). Hydrogen bond and hydrophobic interaction plays the major role in protein – ligand contacts (Figure 6 (C)). There were seven intermolecular hydrogen bonds interactions with the binding site residues GLU190, SER137, VAL135, SER145, GLY134, LYS144 and SER146 that were actively participated during the simulation (Figure 9 and Table 3). The hydrogen atom 68(H) showed a hydrogen bond with oxygen atom OE2 of acidic polar residue GLU190 with a distance of 1.80 Å, the oxygen atom 94(O) indicated a hydrogen bond with HG of polar side chain residue SER137 with a distance of 2.05 Å, the hydrogen atom 67(H) displayed a H-bond with oxygen atom (O) of nonpolar side chain residue VAL135 with a distance of 1.83 Å, the hydrogen atom 89(H) exhibited a H-bond with oxygen atom (O) of polar side chain residue SER145 with a distance of 1.96 Å, the hydrogen atom 85(H) involved in a H-bond with oxygen atom (O) of polar side chain residue GLY134 with a distance of 1.90 Å, the oxygen atom 93(O) participated in a H-bond with HZ1 of basic polar side chain residue LYS144 with a distance of 1.65 Å and the oxygen atom 44(O) displayed a hydrogen bond with HG of polar side chain residue SER:146 with a distance of 2.16 Å. It was discussed in a previous STD NMR study that GM1 and N-acetylneuraminic acid moieties inhibit rotavirus spike protein (35).

Haemagglutinin - KDN dimer connected by CH-N1 nano-spacer complex

The energy profile of the MD trajectroy for the 20ns simulation course is shown in Figure 3 (D). The RMSD of the protein and ligand were evaluated for structural dynamics, and the protein backbone largely fluctuates between the range of 1.0 - 5.0 Å and KDN-CH-N1 Spacer fluctuates along with the protein (Figure 4 (D)). The RMSF of haemagglutinin side chain fluctuates between

the ranges of 0.5 – 6.0 Å (Figure 5 (D)). Hydrogen bond plays the vital role (Figure 6 (D)) in protein – ligand contacts. The binding site residues LEU133, LYS144, SER145, and LYS193 participated in intermolecular hydrogen bonding interactions (Figure 10). The oxygen atom 41(O) formed a H-bond with HZ1 of basic polar side chain residue LYS144 with a distance of 1.66 Å, the hydrogen atom 85(H) showed a hydrogen bond with oxygen atom (O) of polar side chain residue SER145 with a distance of 2.52 Å. In an earlier NMR experiment, sialic acid binds into the binding site residue Ser34 of the agrin-G3 protein domain (36). In addition, the oxygen atom (O) indicated a hydrogen bond with HZ3 of basic polar side chain residue LYS193 with a distance of 2.03 Å and the hydrogen atom 52(H) displayed a H-bond with oxygen atom (O) of nonpolar side chain residue LEU:133 with a distance of 1.95 Å.

Torsion profile

Each rotatable bond (RB) in the ligand conformation inside the binding site is summarized using ligand torsion profile throughout the simulation trajectory of each 20ns. The color coded rotatable bonds in 2D representation of neuraminidase docked analogue KDN dimer coupled by 1-Linker, neuraminidase docked analogue KDN dimer joined by CH-C1 nano-spacer, haemagglutinin docked analogue KDN dimer attached by CH-C1 nano-spacer and haemagglutinin docked analogue KDN dimer CH-N1 nano-spacer are shown in Torsion Profile I, Torsion Profile II, Torsion Profile III and Torsion Profile IV of Figure 11, 12, 13 and 14 respectively. In the Torsion Profile, each rotatable bond is accompanied by a dial (radial) plot and bar plot of the same color. The dial plots illustrate the conformation of the dihedral angle during the course of the simulation. In dial plot, the simulation starts from the middle of the plot and the time progress is radially plotted outwards. The bar plots review the information on the dial plots and shows the probability density of the dihedral angle. In the bar diagram, the potential of the rotatable bond is depicted through torsion potential information. The values of the torsion potential in left Y-axis of the bar chart were expressed in kcal/mol. The torsion potential relationships describe the conformation of the ligand which maintains strong protein-bound conformation.

Avian (H5N1) origin influenza virus causes serious infections to human beings. The pandamic prospective of these viruses must not supposed to be ignored. The two viral proteins namely neuraminidase and haemagglutinin are essential for avian influenza infection. Hence, in the current study, 153 NeuNAc analogues were screened against the mulimeric binding sites of neuraminidase (PDB ID: 2HTQ) and haemagglutinin (PDB ID: 4KDN). Top least five analogues with better interactions into the binding pocket of neuraminidase and haemagglutinin were chosen for further dimeric studies. Homo dimerization was done in which three linkers: 1-Linker, 2-Linker and 3-Linker and five spacers CH-C1, CH-C2, CH-C3, CH-C4 and CH-N1 were used (Figure 1) to join the monomers to form dimers. In total, eighty dimers of NeuNAc analogues were modeled using chemical drawing software ChemSketch. The dimers of NeuNAc analogues were screened against the binding sites of neuraminidase and haemagglutinin using glide docking. The dimers of NeuNAc analogues coupled by nano-spacers fit into the binding site of neuraminidase and haemagglutinin. The dimensions of dimer of KDN coupled by 1-Linker is 2.99nm, dimer of KDN joined by CH-C1 nano-spacer's extent is 2.83nm and size of the dimer of KDN connected by CH-N1 is 2.25nm (Figure 2). The previous spacer study suggests that bolaform cholesterylimide

derivatives were in the size of nm. The CH-C1 xerogel from 1,4-dioxane forms main peaks in the angle with 2θ values of 2.17°, 4.32°, 6.53° and 10.84° the corresponding *d* values of 4.07, 2.04, 1.35, and 0.82 nm respectively (37). The top two analogues with better docking score and energy were found to be for neuraminidase - KDN dimer joined by 1-Linker complex as -15.09 and -48.63 kcal/mol respectively and for neuraminidase - KDN dimer coupled by CH-C1 nano-spacer complex as -15.00 and -66.93 kcal/mol respectively, followed by haemagglutinin - KDN dimer coupled by CH-C1 nano-spacer complex as -11.31 and -56.24 kcal/mol respectively and haemagglutinin - KDN dimer connected by CH-N1 nano-spacer complex as -10.80 and -50.11 kcal/mol respectively. The above said complexes were further analyzed for conformational stability using molecular dynamics simulation. The MD simulation studies revealed that the binding interactions of neuraminidase - KDN dimer joined by 1-Linker complex, neuraminidase - KDN dimer coupled by CH-C1 nano-spacer complex, haemagglutinin - KDN dimer coupled by CH-C1 nano-spacer complex and haemagglutinin - KDN dimer connected by CH-N1 nano-spacer complex were optimally stable with the preferable binding orientations. The conformational analysis using energy trajectory, RMSD, RMSF, Protein – Ligand contact, hydrogen bonding interaction and ligand torsion profile of docked complexes suggests the steady nature of the dimers of NeuNAc analogues into the binding pocket of neuraminidase and haemagglutinin. The active site residues of neuraminidase such as GLU:277, GLU:276, ARG:292, ARG:371, THR:369, SER:370, GLU:432, TYR:347, ARG:152, GLU:119, TYR:406 and haemagglutinin residues such as GLU:190, SER:137, VAL:135, SER:145, GLY:134, LYS:144, SER:146, LYS:193, LEU:133 were involved in direct hydrogen bonding with dimers of NeuNAc analogues during 20ns simulation run. So, this conformational attempt perhaps explains the steady nature of NeuNAc analogue dimers into the binding sites of H5N1 influenza A viral proteins: neuraminidase and haemagglutinin. Therefore NeuNAc analogue dimers may be considered as the futuristic candidates for rational drug design for avian flu.

In conclusion, compare to NeuNAc analogue monomer, NeuNAc analogue dimers show better binding interaction towards the binding pocket of neuraminidase and haemagglutinin. The conformational analysis also maybe suggests the steady nature of the complexes such as, neuraminidase – KDN dimer coupled by 1-Linker complex, neuraminidase – KDN dimer joined by CH-C1 nano-spacer complex, haemagglutinin – KDN dimer linked by CH-C1 nano-spacer complex and haemagglutinin – KDN dimer attached by CH-N1 Spacer complex. The simulation of the dynamic behavior of dimers of NeuNAc analogues reveals that their conformations were flexible inside the binding sites as depicted through the ligand torsion profile which might be responsible for their enhanced binding interaction. Hence, the present design of NeuNAc analogue dimers coupled by nano-spacers may be considered for developing a novel ligand for restraining avian flu infection.

Acknowledgment

The authors acknowledge the computational facility sponsored by SERB (Science and Engineering Research Board, DST) Ref No. (SR/FT/LS-157/2009), Govt. of India, New Delhi.

References

1. Sieben C, Kappel C, Zhu R, Wozniak A, Rankl C, Hinterdorfer P, Grubmüller H, Herrmann A (2012) Influenza virus binds its host cell using multiple dynamic interactions. PNAS 109 (34):

13626–13631
2. Sauter NK, Hanson JE, Glick GD, Brown JH, Crowther RL, Park SJ, Skehel JJ, Wiley DC (1992) Binding of Influenza Virus Hemagglutinin to Analogs of Its Cell-Surface Receptor, Sialic Acid: Analysis by Proton Nuclear Magnetic Resonance Spectroscopy and X-ray Crystallography? Biochemistry 31: 9609-9621
3. Bertozzi CR, Kiessling LL (2001) Chemical glycobiology. Science 291:2357–2364
4. Borman S (2000) Multivalency: strength in numbers. Chem. Eng. News 78:48–53
5. Gestwicki JE, Cairo CW, Strong LE, Oetjen KA, Kiessling LL (2002) Influencing receptor-ligand binding mechanisms with multivalent ligand architecture. J. Am. Chem. Soc 124:14922–14933
6. Griffin JH, Linsell MS, Nodwell MB, Chen Q, Pace JL, Quast KL, Krause KM, Farrington L, Wu TX, Higgins DL, Jenkins TE, Christensen BG, Judice JK (2003) Multivalent drug design. Synthesis and in vitro analysis of an array of vancomycin dimers. J. Am. Chem. Soc 125: 6517–6531
7. Weight AK, Haldar J, Álvarez de Cienfuegos L, Gubareva LV, Tumpey TM, Chen J, Klibanov AM (2011) Attaching Zanamivir to a Polymer Markedly Enhances Its Activity Against Drug-resistant Strains of Influenza a Virus. J Pharm Sci 100:831–835
8. Peiris JSM, de Jong MD, Guan Y (2007) Avian influenza virus (H5N1): a threat to human health. J. Microb. Rev 20:243–267
9. Beigel H, Farrar H, Han AM, Hayden FG, Hyer R, De Jong MD, Lochindarat S, Nguyen TK, Naguyen TH, Tran TH, Nicoll A (2005) Avian influenza A (H5N1) infection in humans. New England Journal of Medicine 353:1374–1385
10. Lee SM, Gardy JL, Cheung CY, Cheung TK, Hui KP, Ip NY, Guan Y, Hancock RE, Peiris JSM (2009) System-level comparison of host-responses elicited by avian H5N1 and seasonal H1N1 influenza viruses in primary human macrophages. PLoS One 4: e8072
11. Cameron CM, Cameron MJ, Bermejo-Martin JF, Ran L, Xu L, Turner PV, Ran R, Danesh A, Fang Y, Chan PM, Mytle N, Sullivan TJ, Collins TL, Johnson MG, Medina JC, Rowe T, Kelvin DJ (2008) Gene Expression Analysis of host innate immune responses during lethal H5N1 infection in ferrets. J Virol 82:11308-11317
12. Matsukura S, Kokubu F, Kubo H, Tomita T, Tokunaga H, Kadukora M, Yamamoto T, Kuroiwa Y, Ohno T, Suzaki H, Adachi M (1998) Expression of RANTES by normal airway epithelial cells after influenza virus A infection. Ann J Respir Cell Mol Biol 18: 255-264
13. Amaro RE, Swift RV, Votapka L, Li WW, Walker RC, Bush RM (2011) Mechanism of 150-cavity formation in influenza neuraminidase. Nature communications 2:388
14. Tong S, Zhu X, Li Y, Shi M, Zhang J, Bourgeoisetal M (2013) New world bats harbor diverse influenza A viruses. PLoS Pathogens 9:1–12
15. Zhu, Xueyong Yu, W, McBride R, Li Y, Chen L-M, Donis RO, Tong S, Paulson JC, Wilson IA (2013) Hemagglutinin homologue from H17N10 bat influenza virus exhibits divergent receptor-binding and pH-dependent fusion activities. Proceedings of the National Academy of Sciences 110:1458-1463
16. Russell RJ, Haire LF, Stevens DJ, Collins PJ, Lin YP, Blackburn GM, Hay AJ, Gamblin SJ, Skehel JJ (2006) The structure of H5N1 avian influenza neuraminidase suggests new opportunities for drug design. Nature 443:45-49
17. Simanek EE, McGarvey GJ, Jablonowski JA, Wong CH (1998) Selectin-carbohydrate interactions: from natural ligands to designed mimics. Chemical Reviews 98:833–862
18. Kiefel MJ, von Itzstein M (2002) Recent advances in the synthesis of sialic acid derivatives and sialylmimetics as biological probes. Chemical Reviews 102:471–490
19. Lengauer T, Rarey M (1996) Computational methods for biomolecular docking. Current Opinion in Structural Biology 6:402–406
20. Lu X, Shi Y, Zhang W, Zhang Y, Qi J, Gao GF (2013) Structure and receptor-binding properties of an airborne transmissible avian influenza A virus hemagglutinin H5 (VN1203mut). Protein & cell 4:502-511
21. Maestro 9.0, (2009) versuib 70110, Schrodinger, New York
22. Kaminski GA, Friesner RA, Tirado-Rives J, Jorgensen WL (2001) Evaluation and reparametrization of the OPLS-AA force field for protein via comparison with accurate quantum chemical calculations on peptides. J. Phys. Chem. B105: 6474–6487
23. Chen IJ, Foloppe NJ (2010) Drug-like bioactive structures and conformational coverage with

the LigPrep/ ConfGen suite: comparison to programs MOE and catalyst. J Chem Inf Model 50:822-39
24. Friesner RA, Banks JL, Murphy RB, Halgren TA, Klicic JJ, Mainz DT, Repasky MP, Knoll EH, Shelley M, Perry JK, Shaw DE, Francis P, Shenkin PS (2004) Glide: a new approach for rapid, accurate docking and scoring. 1. Method and assessment of docking accuracy. J. Med. Chem 47:1739–1749
25. Friesner RA, Murphy RB, Repasky MP, Frye LL, Greenwood JR, Halgren TA, Sanschagrin PC, Mainz DT (2006) Extra Precision Glide: Docking and Scoring Incorporating a Model of Hydrophobic Enclosure for Protein-Ligand Complexes. Journal of medicinal chemistry 49: 6177–6196
26. Shan Y, Kim ET, Eastwood MP, Dror RO, Seeliger MA, Shaw DE (2011) How does a drug molecule find its target binding site? J. Am. Chem. Soc133:9181–9183
27. Essmann U, Perera L, Berkowitz ML, Darden T, Lee H, Pedersen LG (1995) A smooth particle mesh Ewald method. The Journal of Chemical Physics 103:8577
28. Strahan GD, Keniry MA, Shafer RH (1998) NMR structure refinement and dynamics of the K+−(d(G3T4G3))2 quadruplex via particle mesh Ewald molecular dynamics simulations. Biophys. J.75:968–981
29. Ryckaert JP, Ciccotti G, Berendsen HJC (1977) Numerical integration of the cartesian equations of motion of a system with constraints: Molecular dynamics of n-alkanes. Journal of Computational Physics 23:327–341
30. Wright D, Usher L (2001) Multivalent binding in the design of bioactive compounds. Curr. Org. Chem 5:1107–1131
31. Macdonald SJF, Cameron R, Demaine DA, Fenton RJ, Foster G, Gower D, Hamblin JN, Hamilton S, Hart GJ, Hill AP, Inglis GGA, Jin B, Jones HT, McConnell DB, McKimm-Breschkin J, Mills G, Nguyen N, Owens IJ, Parry N, Shanahan SE, Smith D, Watson KG, Wu W-Y, Tucker SP (2005) Dimeric Zanamivir Conjugates with Various Linking Groups Are Potent, Long-Lasting Inhibitors of Influenza Neuraminidase Including H5N1 Avian Influenza. J. Med. Chem 48:2964-2971
32. Fernandez-Alonso MC, Díaz D, Berbis MA, Marcelo F, Canada J, Jimenez-Barbero J (2012) Protein-Carbohydrate Interactions Studied by NMR: From Molecular Recognition to Drug Design. Current Protein and Peptide Science 13:816-830
33. Pell G, Williamson MP, Walters C, Du H, Gilbert HJ, Bolam DN (2003) Importance of Hydrophobic and Polar Residues in Ligand Binding in the Family 15 Carbohydrate-Binding Module from Cell *Vibrio japonicus* Xyn10C. Biochemistry 42:9316-9323
34. Dormitzer PR, Sun Z-Y.J, Blixt O, Paulson JC, Wagner G, Harrison SC (2002) Specificity and affinity of sialic acid binding by the rhesus rotavirus VP8* core. J. Virol 76:10512–10517
35. Fleming FE, Böhm R, Dang VT, Holloway G, Haselhorst T, Madge PD, Deveryshetty J, Yu X, Blanchard H, von Itzstein M, Coulson BS (2014) Relative Roles of GM1 Ganglioside, N-Acylneuraminic Acids, and α2β1 Integrin in Mediating Rotavirus Infection. Journal of Virology 88:4558 – 4571
36. Sallum CO, Kammerer RA, Alexandrescu AT (2007) Thermodynamic and Structural Studies of Carbohydrate Binding by the Agrin-G3 Domain. Biochemistry 46:9541–9550.
37. Jiao T, Gao F, Zhang Q, Zhou J, Gao F (2013) Spacer effect on nanostructures and self-assembly in organogels via some bolaformcholesteryl imide derivatives with different spacers. Nanoscale Research Letters 8:406

How to cite this article:

Jino Blessy, J., D. Jawahar and Jeya Sundara Sharmila, D. 2019. Multivalent Interactions of Nano-spaced Dimers of N-acetylneuraminic Acid Analogues Complex with H5N1 Influenza Viral Neuraminidase and Haemagglutinin - A Molecular Dynamics Investigation. *Int.J.Curr.Microbiol.App.Sci.* 8(01): 1517-1546. doi: https://doi.org/10.20546/ijcmas.2019.801.161